Primary Production in the Arctic Ocean, 1998-2006

Sudeshna Pabi, Gert L. van Dijken, and Kevin R. Arrigo

Department of Environmental Earth System Science, Stanford University, Stanford, CA 94305

Abstract

Sea ice in the Arctic Ocean has undergone an unprecedented reduction in area and thickness in the last decade, exposing an ever-increasing fraction of the sea surface to solar radiation and increasing the habitat suitable for phytoplankton growth. Here we use a primary production algorithm that utilizes remotely sensed chlorophyll *a*, sea surface temperature, and sea ice extent data to quantify interannual changes in phytoplankton production in the Arctic Ocean between 1998 and 2006. Our results show that since 1998, open water area in the Arctic has increased at the rate of 0.07×10^6 km^2 yr^{-1}, with the greatest increases in the Barents, Kara and Siberian sectors, particularly over the continental shelf. Although pan-Arctic primary production averaged 419±33 Tg C yr^{-1} during 1998-2006, recent increases in open water area have lead to higher rates of annual production, which reached a nine-year peak in 2006. Annual production was roughly equally distributed between pelagic waters (less productive but greater area) and waters located over the continental shelf (more productive but smaller area). Interannual differences are most tightly linked to changes in sea ice extent, with changes in sea surface temperature (related to the Arctic Oscillation) and incident irradiance playing minor roles. Estimation of primary production in the Arctic will aid the assessment of air-sea CO_2 fluxes and improve our understanding of the ecological and biogeochemical changes that could take place if ice cover continues to decrease.

1. Introduction

The Arctic Ocean is currently in the forefront of climate change caused by both natural and anthropogenic factors. Since 1950, the mean annual air temperature has increased by 2-3°C and by 4°C in winter [*Chapman and Walsh*, 2003], resulting in markedly longer summers [*Smith*,

1998]. Temperature is projected to increase by an additional 4-5°C by the end of the 21st century [*ACIA, 2005*]. In conjunction with these higher temperatures, sea ice cover in the Arctic Ocean has been contracting over the past three decades, with dramatic reductions in recent years [*Levi*, 2000; *Parkinson*, 2000]. Changes in sea ice cover also include an increase in the length of the ice melt season [*Smith*, 1998; *Rigor et al.*, 2002; *Serreze et al.*, 2007; *Comiso et al.*, 2008] and a decrease in ice thickness over the central Arctic Ocean [*Rothrock et al.*, 1999]. The result is greater open water area and enhanced shelf break upwelling, the latter of which is expected to increase the input of nutrients from offshore waters to shallower shelves [*ACIA, 2005*]. While a reduction in sea ice should favor the growth of phytoplankton and increase the net air-to-sea flux of CO_2 [*Anderson and Kaltin*; 2001; *Bates et al.,* 2006], it also will reduce the amount of production contributed by algae growing within the sea ice [*Subba Rao and Platt*, 1984; *Legendre et al*., 1992; *Gosselin et al*., 1997], although sea ice communities generally account for a relatively small fraction of total primary production in Arctic waters.

One step towards a better understanding of the effects of these environmental changes on the marine ecosystem and carbon biogeochemistry in the Arctic is to quantify current rates of basin-scale phytoplankton primary production. While a number of primary production estimates are already available for the Arctic [e.g., *Platt et al.,* 1982; *Wassman and Slagstad,* 1993; *Vedernikov et al.*, 1995; *Gosselin et al.,* 1997; *Boetius and Damm*, 1998; *Tremblay et al.,* 2002], these cover relatively small temporal and spatial scales. This is primarily due to the difficulty of sampling such a harsh and often inaccessible environment. The data that are available suggest that rates of primary production in this region are governed by its unique physical environment. For example, the shallow bathymetry of much of the Arctic Ocean greatly influences the light and nutrient inventories that are required for primary production. Discharge from rivers both enhances primary production by supplying additional nutrients and inhibits it by limiting light transmission through the water column due to high sediment loads [*Kirk*, 1983]. Sea ice also impacts light transmission to the water column and plays a crucial role in determining the mixed layer depth (via increased stratification during ice melt and convective mixing during sea ice

55 formation) that, along with the critical depth, dictates the onset and demise of the spring and
56 summer phytoplankton blooms.
57 Unlike other oceans, the Arctic Ocean is almost completely landlocked, except for the very
58 shallow Bering Strait (~50 m), that connects it to the Pacific Ocean, and the Fram Strait and
59 Canadian Archipelago that allow exchange with the Atlantic Ocean. Associated with the
60 extensive land margin is a broad continental shelf. Extending over an area of 5×10^6 km^2, the
61 continental shelf comprises about 53% of total Arctic Ocean area, much higher than the 9.1 -
62 17.7% characteristic of continental shelves in other oceans of the world [*Menard and Smith*,
63 1966; *Jakobsson*, 2003]. Ice-free continental shelves, such as those found in parts of the
64 Chukchi Sea, often experience intense seasonal blooms of phytoplankton owing to their
65 favorable nutrient and light conditions [*Hill and Cota*, 2005].
66 Another unique feature of the Arctic Ocean is the large amount of riverine discharge it
67 receives (~4000 km^3 yr^{-1}) [*Shiklomanov*, 2000; *Carmack and Macdonald*, 2002], arising from
68 both large rivers, like the Ob, Lena, Yenisey, and Mackenzie, and numerous smaller ones in both
69 the Amerasian and Eurasian sectors. This large freshwater input affects both the salinity and
70 nutrient concentration of the Arctic Ocean. Furthermore, it is predicted that precipitation in a
71 warming climate will increase significantly [*IPCC*, 2006], thereby enhancing the already
72 enormous fluxes of riverine sediment discharge (670 Mt yr^{-1}) and organic carbon (12.6 Mt yr^{-1})
73 from the land to the Arctic Ocean [*Macdonald et al.*, 1998], both of which will impact nutrient
74 and light availability and hence, phytoplankton growth.
75 The circulation of the Arctic Ocean is comprised of both low salinity (<33) and nutrient-rich
76 Pacific Ocean water and relatively nutrient-poor and more saline (~34.8) Atlantic Ocean water
77 [*Maslowski et al.*, 2004]. The denser Atlantic water is distributed via counterclockwise currents
78 along the continental slope at the basin margins. The relatively less saline and warmer Pacific
79 water enters the Arctic Basin through the Bering Strait between Cape Dezhnev and west Alaska,
80 and exits through the Canadian Archipelago, the Fram Strait and the Nares Strait. Historically,
81 the front separating the Atlantic and Pacific water has been located over the Lomonosov Ridge,

but recently this front appears to have moved closer to the Alpha-Mendeleev Ridge. This shift in the location of the front has lead to the displacement of a large quantity of Pacific water that has been replaced by nutrient-poor water from the Atlantic [*Macdonald*, 1996], potentially reducing the amount of nutrients available for phytoplankton growth. The nutrient-rich water from the Pacific Ocean is generally restricted to the Chukchi Sea and the Amerasian Basin [*Carmack et al.,* 1997].

Surface concentrations of nitrate, phosphate and silicic acid in Arctic waters approach detection limits after the spring bloom [*Sakshaug*, 2003], suggesting that annual primary production is generally controlled by nutrient availability. The nitrate to phosphate ratio in these waters ranges from 11 to 16 (mol:mol) [*Sakshaug*, 2003], suggesting that much of the Arctic Ocean is nitrogen-limited (assuming that phytoplankton require nitrogen and phosphorus at the Redfield ratio of 16:1). Phosphorus limitation of phytoplankton is more likely in waters with a salinity of <25 [*Sakshaug et al.,* 1983] due to low phosphate content of river waters that are otherwise rich in nitrate. The silicic acid to nitrate molar ratio is spatially variable, ranging from a high of 1.9-2.4 in the Chukchi Sea and Eastern Canadian Arctic to a low of 0.31 in the Eurasian basin [*Codispoti*, 1979; *Harrison and Cota,* 1991; *Sakshaug*, 2003].

Finally, sea ice dynamics are integral to the regulation of primary production in much of the Arctic Ocean. In winter, brine rejection due to ice formation destabilizes the mixed layer, leading to deep vertical mixing and replenishment of surface nutrient inventories. In spring, melting of ice results in strong surface ocean stratification, exposing the nutrient-rich waters to a light regime suitable for phytoplankton growth. The resulting spring ice edge bloom forms a significant component of the annual primary production [*Niebauer et al.*, 1990; *Falk-Petersen et al.*, 2000]. In the study presented here, we assessed seasonal and interannual changes in the physical characteristics of the Arctic Ocean, including changes in irradiance, sea surface temperature, and sea ice distributions. In addition, we quantified the changes in phytoplankton chlorophyll *a* (Chl *a*) and primary production that accompanied interannual differences in the physical environment of the Arctic Ocean within a number of different ecological provinces

(e.g., pelagic, continental shelf, etc.). This was accomplished using a primary production algorithm parameterized for the Arctic Ocean with input data from a number of satellite remote sensing platforms. This approach has the advantage of providing estimates of Arctic primary production at relatively high temporal resolution over large geographic areas.

2. Methods

2.1. Primary Production Algorithm

Daily primary productivity (*PP*, mg C m^{-2} d^{-1}) at each satellite pixel location was computed by integrating over depth *z* (0-100 m at 1 m intervals) and time *t* (hourly for 24 hours) as described in detail in *Arrigo et al.* [1998] and modified by *Arrigo et al.* [2008]. In its simplest form, the governing equation can be represented as:

$$PP = \int_{z=0}^{100} \int_{t=0}^{24} Chl(z) \frac{C}{Chl} G(z,t) dt\, dz \qquad (1)$$

where $G(z,t)$ is the net biomass-specific phytoplankton growth rate (hr^{-1}) and C/Chl is the phytoplankton carbon to Chl *a* ratio (90 g:g, see below). Surface Chl *a* concentrations determined from 8-day SeaWiFS L3 images are considered to be representative of concentrations throughout the mixed layer. Below the mixed layer, Chl *a* is assumed to decrease exponentially with depth as described by *Arrigo et al.* [2008]. In the Arctic, the spring-summer mixed layer depth (MLD) is reported to vary between 15 m and 20 m [*McLaughlin et al*., 2002]. In the present study, the MLD is assumed to be 20 m, similar to the value used by *Walsh et al.* [2005]. Sensitivity studies revealed that the algorithm is not sensitive to MLD; for example, increasing the MLD to 50 m increased the calculated depth-integrated primary production by only 10%. $G(z,t)$ is calculated each hour (t) and at each depth (z) as a function of the temperature-dependent upper limit to net growth and a light limitation term, *L* (dimensionless):

$$G(z,t) = G_o \exp[rT(z)]\, L(z,t). \qquad (2)$$

where G_o is the maximum microalgal net growth rate at 0°C (0.59 d^{-1}) and r is a rate constant (0.0633 $°C^{-1}$) that determines the sensitivity of G to temperature, T (°C) [*Eppley*, 1972]. The light limitation term, $L(z,t)$, is calculated for each depth and each hour as

$$L(z,t) = 1 - \exp\left(-\frac{PUR(z,t)}{E_k'(z,t)}\right) \quad (3)$$

where $PUR(z,t)$ is photosynthetically usable radiation [*Morel*, 1978; 1987; 1991] and $E_k'(z,t)$ is the spectral photoacclimation parameter [*Arrigo and Sullivan*, 1994]. *PUR* is similar to photosynthetically active radiation (PAR, the total radiation between 400 and 700 nm), except that *PUR* is weighted by the phytoplankton specific absorption spectra, as described by *Morel* [1978], and represents the subset of PAR that is readily absorbed by phytoplankton. $E_k'(z,t)$ varies with light history, simulating phytoplankton photoacclimation to a changing light regime. Downwelling spectral irradiance at the ocean surface was determined using the radiative transfer model of *Gregg and Carder* [1990], corrected for fractional cloud cover (from NCEP Reanalysis data) and specular reflectance [*Arrigo et al*., 2008]. Downwelling spectral irradiance was propagated through the water column according to Beer's law as described in *Arrigo et al.* [1998] using the inherent optical properties typical of this ocean [*Wang and Cota*, 2003].

2.2. Algorithm Input Data

Chlorophyll a: Surface Chl *a* concentrations were determined from Level 3 (9 km resolution) SeaWiFS ocean color data (operational August 1997-present, distributed by http://oceancolor.gsfc.nasa.gov/) using the OC4v4 algorithm [*O'Reilly et al.*, 1998]. The OC4v4 Chl *a* algorithm is suitable for Case I waters where the optical properties are dominated primarily by Chl *a*. However, we recognize that a large sediment load as well as CDOM from river discharge has the potential to alter these optical properties and impact Chl *a* retrievals. Hence, to account for the influence of riverine sediments in coastal waters, primary production was quantified both by including and excluding questionable SeaWiFS pixels that were in proximity to the river discharge plumes (these pixels were flagged as being turbid in the SeaWiFS data).

Because exclusion of pixels associated with river discharge reduced the pan-Arctic primary production by less than 10%, all results reported here have had river-influenced pixels removed.

In addition, SeaWiFS data for the Arctic Ocean are only available from March through September, after which the SeaWiFS sensor begins focusing its data collection and storage on more southerly waters. Because irradiance is minimal outside this data collection period, the lack of SeaWiFS data at other times of year is likely to result in only a slight underestimate of annual primary production (<10%).

Sea Surface Temperature: Sea surface temperature (SST) is based on the Reynolds Optimally Interpolated SST (OISST) Version 2 product [*Reynolds et al*., 2002] obtained from NOAA (http://www.emc.ncep.noaa.gov/research/cmb/sst_analysis/).

Open Water Area: Open water area was estimated from Special Sensor Microwave Imager (SSM/I) 37 and 85 GHz bands using the Polynya Signature Simulation Method (PSSM) algorithm [*Markus and Burns*, 1995] which allows determination of sea ice presence/absence at 6.25 km resolution. A given pixel is defined as being ice covered wherever the sea ice concentration is greater than approximately 10%.

All satellite remote sensing data were processed using Interactive Data Language (IDL). The primary productivity algorithm was encoded using Fortran 77. All computations were done at the High Productivity Technical Computing facility of Stanford's Center of Computational Earth and Environmental Science, which is composed of a Sun Sparc cluster running Solaris 10.

2.3. Defining Regions of Interest

The Arctic Ocean is defined as all waters north of the Arctic Circle (66° 33' 39"). For the purpose of characterizing spatial differences, we divided the Arctic Ocean into eight geographic sectors and four open-water ecological regimes. The geographic sectors were demarcated by longitude (Fig. 1a) and include the Chukchi (180° to 160°W), Beaufort (160°W to 100°W), Baffin (100°W to 45°W), Greenland (45°W to 15°E), Barents (15°E to 55°E), Kara (55°E to 105°E), Laptev (105°E to 150°E), and Siberian (150°E to 180°) sectors.

186 The four ecological provinces include the pelagic, the shelf, the deep water marginal ice zone
187 (DMIZ) and the marginal ice zone (MIZ) over the continental shelf (SMIZ). All provinces vary
188 in size over time due to continual changes in sea ice extent (Fig. 1b). The ecological provinces
189 were demarcated using a combination of sea ice distributions and bathymetric information. The
190 pelagic and shelf provinces are defined as those waters with depths of >220 m and ≤220 m,
191 respectively (in accordance with the definition of the Arctic continental shelf by *Walsh et al.,*
192 2005), and that have remained ice-free for >14 consecutive days. A pixel is considered part of
193 the MIZ if it has been ice-free for ≤14 days [*Arrigo et al*., 2008]. If an MIZ pixel is located on
194 the shelf, then it is defined as belonging in the SMIZ, otherwise it is defined as being part of the
195 DMIZ. The SMIZ and DMIZ together constitute the total Arctic Ocean MIZ.
196
197 **2.4. Algorithm Validation**
198 In the present study, we chose to use the surface Chl *a* concentrations produced from
199 SeaWiFS data by the standard OC4v4 algorithm [*O'Reilly et al*., 1998] rather than the regional
200 Arctic algorithm of *Wang and Cota* [2003]. This decision was based on a recent assessment by
201 *Matsuoka et al.* [2005], who used measurements of in-water apparent optical properties and Chl
202 *a* to show that the standard OC4v4 Chl *a* algorithm used with SeaWiFS data performs as well or
203 better in Arctic waters than the algorithm of *Wang and Cota* [2003]. The two algorithms
204 exhibited root mean square (RMS) errors between *in situ* and satellite-derived Chl *a* of 25% and
205 30%, respectively.
206 The best way to validate our primary production algorithm would be to compare algorithm-
207 derived production with *in situ* estimates of primary production made at the same time and
208 location. However, because of the small number of cloud-free images that correspond to
209 available *in situ* measurements in the Arctic, this approach is not feasible. Thus, to validate our
210 primary production algorithm we assumed that retrievals of surface Chl *a* by SeaWiFS were
211 reliable (in waters not influenced by river runoff) and then compared regressions of daily

primary production against surface Chl *a* produced by our algorithm to similar regressions generated from *in situ* Arctic data.

In situ measurements of primary production and concurrent surface Chl *a* concentrations used in this analysis were obtained from Phase I and II of the Shelf Basin Interaction (SBI) program [*http://www.eol.ucar.edu/projects/sbi/*] conducted in the Chukchi and Beaufort sectors of our study area during 2002-2004. The relationship between surface Chl *a* and daily primary production predicted by our algorithm for the SBI study region agrees well with the *in-situ* data, particularly in spring (Fig. 2a). In summer, there are clear cases where the algorithm underestimates daily production at low surface Chl *a* concentrations (Fig. 2b). These were stations with a particularly strong subsurface Chl *a* maximum [*Hill and Cota*, 2005], which was not detected by the SeaWiFS sensor. Unfortunately, the prevalence of subsurface Chl *a* maxima in the Arctic Ocean is not well known so the significance of the problem cannot be adequately determined at this time.

The relationship between surface Chl *a* and computed primary production is sensitive to the value used for the C:Chl *a* ratio. A value of 90 produced the best agreement between algorithm-derived and *in situ* primary production. This is encouraging because 90 is similar to the C:Chl *a* ratio determined to be optimal for computing primary production in the Southern Ocean (88.5) using the same algorithm as that used here [*Arrigo et al.*, 2008]. It is also well within the range of 25-100 reported for *in situ* C:Chl *a* measurements from the Arctic [*Platt et al.*, 1982; *Buck et al.*, 1998; *Sakshaug*, 2003]. Although the paucity of Arctic data makes it difficult to validate our algorithm across the full range of surface Chl *a* values that have been measured, our algorithm has been validated over a much larger range of Chl *a* concentrations and rates of daily primary production in the Southern Ocean [*Arrigo et al.*, 2008], further supporting its use in northern polar waters.

3. Results

3.1 Interannual Ice Dynamics

3.1.1. Pan-Arctic

During the 9-year period of interest (POI) of this study (1998-2006), the annual mean open water (ice-free) area in the Arctic Ocean exhibited a dramatic and statistically significant upward trend (R^2=0.78, p= 0.002), increasing at the rate of ~0.07×10^6 km^2 yr^{-1} (Fig. 3a). This trend is consistent with earlier studies reporting a substantial loss of sea ice in recent decades, with Arctic ice cover decreasing by ~0.80×10^6 km^2 (7.4%) between 1978 and 2002 [*Johannessen et al.*; 1999; *Cavalieri et al.*, 2003]. Open water area during the POI was at its nine-year low in 1998, averaging ~3.8×10^6 km^2 over the year; the maximum annual mean open water area was attained in 2006, averaging 4.6×10^6 km^2. Although annual mean open water area in the Arctic increased by 19% between 1998 and 2006, this increase was not uniform throughout the year. For example, during August-September (the peak open water season, Fig. 4a), open water area averaged $6.9 \pm 0.03 \times 10^6$ km^2 during the POI, and increased by 11% between 1998 and 2006 (Fig. 3c). However, during May-June (the peak of the spring phytoplankton bloom), open water area averaged only $3.3 \pm 0.02 \times 10^6$, but the change over time was more pronounced than in summer, increasing by 26% between 1998 and 2006 (Fig. 3b). This pattern reflects the fact that in recent years, Arctic sea ice has been retreating progressively earlier in the year.

Recent increases in annual mean open water area in the Arctic are the result of changes in both the timing of sea ice advance and retreat (earlier retreat and later advance will result in higher annual mean open water area) and the maximum amount of open water area attained during the year. For example, the relatively large annual mean open water area observed in 2002 and 2005 were due mainly to the extensive open water area in summer. On the other hand, open water area 2006 (the lightest sea ice year) was actually lower in the summer than it was in several of the preceding years (1999, 2002 and 2005) (Fig 3c). However, the retreat of sea ice began relatively early in 2006 and the advance began later (Fig. 4a), more than compensating for the low summertime open water area. The early retreat of sea ice in recent years appears to be

coupled with the higher early season SST, particularly in 2005 and 2006 (Fig. 4b). The annual mean SST in the Arctic Ocean increased from -0.07°C in 1998 to +0.26°C in 2006. Unfortunately, it is not clear from these data whether higher SST led to the increase in open water area or vice-versa. However, the peak in SST (Fig. 4b) correlates well with the timing of peak open water area (Fig. 4a), with the latter lagging the annual SST peak by approximately 20 days.

3.1.2. Geographic Sectors

Among all geographic sectors, the Greenland and Barents had the largest annual mean open water area, averaging ~1.6±0.36 × 10^6 km^2 and ~1.1±0.11 × 10^6 km^2, respectively (Fig. 5) during the POI. Whereas open water area in most sectors was reduced to near zero in winter, the Barents and Greenland sectors had significant amounts of permanently open water (Fig. 14c), which appears to have increased in the Barents sector in recent years. The lowest annual mean open water area in the Arctic was observed in the Siberian and Laptev sectors, averaging only 0.18±0.06 × 10^6 km^2 and 0.22±0.06 × 10^6 km^2, respectively. Interannual differences in annual mean open water area were most dramatic in the Eurasian sectors, with the annual mean open water area in the Siberian, Laptev and Kara sectors being 206%, 134%, and 114% higher, respectively, in their lightest sea ice year than in their heaviest.

Over the POI, the rate of change in open water area varied substantially by geographic sector (Fig. 5). The Barents, Kara and Siberian sectors experienced greater absolute increases in open water area than any other sector, with the annual mean open water area increasing at a rate of 25,047 km^2 yr^{-1} (about 2% of the 1998 extent), 20,046 km^2 yr^{-1} (about 10% of the 1998 extent), and 14,416 km^2 yr^{-1} (about 30% of the 1998 extent), respectively, over the POI, although this increase was only statistically significant in the Siberian sector. In other sectors, open water area increased at a rate of only ~5,000 km^2 yr^{-1} (except for the Beaufort, where open water area decreased over time). The relative increase in open water area was largest in the Siberian sector, increasing 276% between 1998 (0.05× 10^6 km^2) and 2005 (0.19× 10^6 km^2). In terms of absolute

291 area, the Barents sector experienced the largest rise in open water area, increasing by 0.36×10^6
292 km^2 between 1998 and 2006. Despite having the largest open water area of all the geographic
293 sectors, changes in open water area in the Greenland sector were far less dramatic, with the
294 minimum and maximum open water years (1998 and 2004, respectively) differing by only 7%.
295 This small change is due to a large area of permanently open water within the pelagic province
296 that has persisted throughout the POI. Interestingly, open water area in the Beaufort sector
297 actually dropped during the POI, decreasing by 178% over the 9-year study period, from a
298 maximum area of 0.38×10^6 km^2 in 1998 to a minimum of 0.12×10^6 km^2 in 2001. However,
299 this trend was dominated by the large drop in ice cover between 1998 and 1999 (Fig. 5c). Since
300 then, interannual changes in open water area in the Beaufort have been small.
301
302 **3.1.2. Ecological Provinces**
303 **3.1.2.1. Annual Mean Open Water Area**
304 *Pelagic*. The largest ecological province in the Arctic Ocean is the pelagic, encompassing an
305 annual mean area of $2.16 \pm 0.07 \times 10^6$ km^2 during the POI (Fig. 5a). In the Greenland and the
306 Barents sectors, the pelagic province comprises 82% (1.34×10^6 km^2) and 47% (0.53×10^6 km^2),
307 respectively, of the total open water area in these sectors (Fig. 5e and f). The Baffin and
308 Beaufort sectors also have significant pelagic provinces, covering 45% (0.18×10^6 km^2) and
309 25% (0.05×10^6 km^2), respectively, of their total area during the POI (Figs. 5c and d).
310 *Shelf*. The shelf province is the second largest ecological province in the Arctic Ocean with
311 an annual mean open water area of $0.90 \pm 0.1 \times 10^6$ km^2 (Fig. 5a). The two geographic sectors
312 with the largest shelf province (in absolute area) were the Barents and Chukchi (Fig. 5b and f),
313 where open water area averaged 0.37×10^6 km^2 (32% of annual mean open water area in that
314 sector) and 0.12×10^6 km^2 (59% of annual mean open water area in that sector), respectively,
315 during the POI. Other geographic sectors with substantial shelf provinces were the Siberian,
316 Laptev, and Kara sectors, where the shelf comprised 47% (0.05×10^6 km^2), 46% (0.07×10^6

317 km^2), and 39% (0.12 × 10^6 km^2), respectively, of total open water area in their respective sectors
318 during the POI.

319 *SMIZ*. The area of the SMIZ province was slightly smaller than the shelf province, with an
320 annual mean open water area of 0.70 ± 0.04 × 10^6 km^2 (Fig. 5a). Geographic sectors with a
321 relatively large SMIZ include the Siberian, Laptev, Kara and Chukchi sectors, where the SMIZ
322 was nearly as large as the shelf province, averaging 49% (0.05 × 10^6 km^2), 44 % (0.06 × 10^6
323 km^2), 41% (0.12 × 10^6 km^2) and 31% (0.06 × 10^6 km^2), respectively, of total open water area
324 during the POI. The largest SMIZ in terms of absolute area was in the Barents sector, averaging
325 0.16 × 10^6 km^2, although it comprised only 14% of the total open water area in that sector.

326 *DMIZ*. The DMIZ is the smallest of the four ecological provinces, averaging just 0.43 ± 0.04
327 × 10^6 km^2 over the POI (Fig. 5a). The DMIZ was largest in the Greenland sector, where it
328 averaged 0.19 × 10^6 km^2, nearly 50% of the total DMIZ area of the Arctic. This province was
329 also relatively large in the Beaufort sector (0.08 × 10^6 km^2), where it comprised 27% of the open
330 water area, and in the Barents (0.05 × 10^6 km^2) and Baffin sectors (0.07 × 10^6 km^2) where it
331 comprised 17% of open water area.

332

333 **3.1.2.2. Changes Over Time**

334 *Annual cycle*. Open water area in the pelagic province of the Arctic Ocean typically increases
335 from a winter low of 1.2-1.7 × 10^6 km^2 (range reflects values for different years) to a peak of 3.2-
336 3.6 × 10^6 km^2 some time between late August and late October (Fig. 6). Winter ice cover is
337 much heavier in the other ecological provinces, such as the shelf, where open water area
338 increased by an order of magnitude from a January minimum of only 0.12-0.30 × 10^6 km^2 to a
339 maximum of 2.4-3.4 × 10^6 km^2 in early September to late October. The open water area in the
340 SMIZ and DMIZ increased even more dramatically, rising seasonally by two orders of
341 magnitude, from a low of 0.02-0.09 × 10^6 km^2 and 0.01-0.07 × 10^6 km^2, respectively, in January
342 to a peak of 2.1-2.6 km^2 and 1.2-2.5 × 10^6 km^2, respectively, during the peak open water period

(mid-July to early September). The length of the open water period in the shelf, SMIZ, and DMIZ provinces were in general shorter than that of the pelagic province.

Interannual trends. The annual mean open water area in the pelagic province of the Arctic increased annually at a rate of 0.17×10^6 km^2 yr^{-1} (R^2= 0.42) between 1998 and 2006, although this increase is not statistically significant (p=0.06, Table 1). Although smaller in area, the secular increase in annual mean open water area during the POI in both the shelf and the SMIZ provinces was significant, increasing annually at a rate of 0.05×10^6 km^2 yr^{-1} (R^2 = 0.77, p=0.002) and 0.01×10^6 km^2 yr^{-1} (R^2 = 0.55, p=0.02), respectively (Table 1). Secular increases in open water area were most dramatic in the shelf and the SMIZ zones of the Siberian sector (Table 1), increasing at a rate of 0.010×10^6 km^2 yr^{-1} (R^2 = 0.64, p=0.01) and 0.004×10^6 km^2 yr^{-1} (R^2 = 0.75, p=0.02), respectively, during the POI (Table 1). These changes in the Siberian sector represent a 9-fold increase in open water area (from a minimum of 0.012×10^6 km^2 in 1998 to maximum of 0.110×10^6 km^2 in 2005) in the shelf and a 2-fold increase (from a minimum of 0.033×10^6 km^2 in 1998 to maximum of 0.067×10^6 km^2 in 2005) in the SMIZ province between 1998 and 2006 (Fig 5i). Apart from these regions, there was no significant secular increase in open water area within the ecological provinces of any geographic sector of the Arctic during the POI (Table 1).

3.2. Primary Production

3.2.1. Pan-Arctic Primary Production

Phytoplankton dynamics in the Arctic Ocean are characterized by an initial spring bloom in April-May, and in some years, a subsequent summer bloom during July-August (Fig. 7a). Between these two blooms, mean surface Chl *a* concentrations in the Arctic remain relatively high, generally exceeding 1.5 mg m^{-3}. Surprisingly, the summer bloom was the more prominent of the two blooms during the first half of the POI (1998-2001), with the mean Chl *a* concentration during summer bloom being comparable to or even exceeding that measured during spring. Between 2002 and 2004, this pattern was reversed, with Chl *a* concentrations in

370 spring exceeding those in both summer and autumn. However, in the two most recent years, the
371 intensity of the summer bloom had again increased, with Chl *a* concentrations eclipsing those of
372 the spring bloom in both 2005 (by a large margin) and 2006 (only slightly).
373 The daily rate of area-normalized production over the entire Arctic basin during the POI
374 averaged 420±26 mg C m^{-2} d^{-1} during the phytoplankton growing season from March through
375 September. Rates were highest in 2006 and 2001, averaging 474 and 447 mg C m^{-2} d^{-1},
376 respectively (Fig. 7a). The mean daily rate of area-normalized production was lowest in 1999 at
377 393 mg C m^{-2} d^{-1}. The daily rate of area-normalized production peaked during the May-June
378 period (Fig. 7c), correlating well with surface Chl *a* (Fig. 7a) during the spring bloom when the
379 amount of PAR incident on the sea surface is relatively high (Fig. 7b). Despite occasionally high
380 Chl *a* concentrations (Fig. 7a), daily area-normalized rates of production (Fig. 7c) were
381 consistently lower during the summer months because of the dwindling irradiance characteristic
382 of this time of year (Fig. 7b).
383 Although daily production in August-September (360±33 mg C m^{-2} d^{-1}) was lower than in
384 May-June (659±39 mg C m^{-2} d^{-1}), the August-September values have a disproportionate impact
385 on annual primary production (Fig. 7d) because they coincide with the annual peak in open water
386 area (Fig. 4a). For instance, 2001 exhibited the highest August-September rates of area-
387 normalized production of any year except 2006 (Fig. 7c). Because this high rate of area-
388 normalized production coincided with the annual peak in open water area, annual production in
389 2001 was among the highest of any year during the POI (Fig. 8a), even though open water area
390 was below average (Fig. 3a). On the other hand, high rates of area-normalized production in
391 May-June do not necessarily translate into high annual area-integrated production. For example,
392 in 2003, a high daily rate of area-normalized production during May led to high total production
393 during this month (Fig. 7d), but the annual production was still relatively low (Fig. 8a) because
394 of depressed August-September values (Fig. 7c). In 2006, the relatively high open water
395 conditions earlier in the year (Fig. 4a), coupled with a high area-normalized primary production

396 rate (Fig. 7c), led to high total production throughout the productive period of the year (Fig. 8b),
397 and therefore the highest annual production (Fig. 8a) during the POI.
398 Annual pan-Arctic primary production averaged 419±33 Tg C yr^{-1} during 1998-2006 (Fig.
399 8a), with an interannual variability of 26% [(max-min)/mean]. Annual production peaked in
400 2006 at 483 Tg C yr^{-1} and was lowest in 1998 at 375 Tg C yr^{-1}. Overall, total Arctic primary
401 production increased during 1998-2006, but not significantly (R^2=0.4, p=0.07), increasing each
402 year by an additional 7.62 Tg C yr^{-1}. The relatively low coefficient of determination (R^2)
403 between annual primary production and year is due to a period of decreased production between
404 2001 and 2003. This transient decrease in annual production is largely attributable to a drop in
405 productivity during the months of August-September between 2001 and 2004 (Fig. 8c). While
406 total production during the two months of the spring bloom (May-June) (Fig. 8b) exhibited a
407 markedly increasing temporal trend, rising at the rate of 4.57 Tg C yr^{-1} (R^2=0.6, p=0.01), there
408 was no significant interannual trend in production during the period of maximum open water
409 area (August-September) (Fig. 8c).
410
411 **3.2.2. Geographic Sectors**
412 Annual primary production in the Arctic varied widely between geographic sectors (Fig. 9).
413 The two largest sectors, the Greenland and Barents, also were the most productive (Figs. 9e and
414 f), averaging ~133 Tg C yr^{-1} and 108 Tg C yr^{-1}, respectively. Even though the Greenland and
415 Barents sectors did not have the highest area-normalized production rate, the large seasonal and
416 perennial open water area in these regions (Fig. 5) resulted in high total annual production. Most
417 of the other geographic sectors exhibited much lower rates of annual production during the POI,
418 generally in the range of 25-50 Tg C yr^{-1}. Annual production was lowest in the Siberian sector,
419 which averaged only ~17.8 Tg C yr^{-1} during the POI (Fig. 9i).
420 The degree of interannual variability in annual primary production also was quite high
421 between sectors (Fig. 9). The Greenland sector exhibited the least amount of variability (Fig.
422 10e), as determined from its low coefficient of variation (CV=standard deviation/mean) of 0.05.

423 The Baffin, Barents, and Chukchi sectors exhibited an intermediate amount of interannual
424 variability, with CVs for annual primary production all ranging from 0.10 to 0.15. The highest
425 amount of interannual variability was observed in the Beaufort, Kara, Laptev, and Siberian
426 sectors, which had CVs in the range of 0.24-0.29. In most sectors, yearly changes in annual
427 primary production (Fig. 9) can be explained by interannual changes in sea ice cover (Fig. 5),
428 with most geographic sectors exhibiting a significant correlation between these two quantities
429 (Table 2). In fact, the sectors with the highest correlation between annual production and open
430 water area (Beaufort, Barents, Kara, Laptev, and Siberian) were also the sectors with the highest
431 degree of interannual variability in annual primary production. The unusually slight variation in
432 annual production in the Greenland sector and the lack of a relationship with open water area
433 was most likely due to the presence of a large area of permanently open water that varied little
434 interannually.
435 The Siberian was the only Arctic sector that exhibited a significant increase in annual
436 primary production during the POI ($R^2 = 0.6$, $p=0.009$), rising each year at the rate of 1.7 Tg C
437 yr^{-1} (Table 3). Most other sectors displayed either no obvious temporal trend between 1998 and
438 2006 or a slight, but non-significant increase (Fig. 9). The Beaufort was the only sector where
439 annual production actually decreased during the POI, falling each year at a rate of 1.5 Tg C yr^{-1}
440 ($R^2 =0.4$, $p=0.059$). However, this negative trend was not statistically significant, being driven
441 primarily by large decreases in production during the first two years of the POI (Fig. 9).
442 Between 2000 and 2006, annual production in the Beaufort remained relatively constant.
443
444 **3.2.3. Ecological Provinces**
445 **3.2.3.1. Pelagic**
446 Among the ecological provinces of the Arctic, total annual production was highest in the
447 pelagic province (Fig. 9a), averaging 154 ± 13 Tg C yr^{-1} during the POI, which constituted 34-
448 40% of pan-Arctic annual primary production. The high annual production in this province is
449 due to its large open water area, accounting for ~52% of the average open water area in the entire

Arctic basin over a year. The pelagic province was the dominant contributor to annual production in the Greenland and the Barents sectors (Figs. 9e and f), where it accounted for 75% (98 Tg C yr^{-1}) and 35% (37 Tg C yr^{-1}), respectively, of total annual production. There was no significant temporal trend in annual production in the pelagic province, either for the entire Arctic Ocean or within individual geographic sectors. The area-normalized production rate in the pelagic province was lower than that of the shelf and the SMIZ provinces (Fig. 10), averaging 348±22 mg C m^{-2} d^{-1}, and exhibiting no interannual trend during the POI. The area normalized production rate in the pelagic province reached its yearly maximum of 781-1016 mg C m^{-2} d^{-1} between April and mid-July (Fig. 10).

3.2.3.2. Shelf

Annual primary production in the shelf province averaged 86 ± 14 Tg C yr^{-1} during the POI (Fig. 9a), contributing 16-24% of pan-Arctic production. The shelf province was particularly important in the Barents, Kara, and Chukchi sectors (Fig. 9), where it accounted for 31% (33±8 Tg C yr^{-1}), 32% (12±4 Tg C yr^{-1}), and 41% (10±2 Tg C yr^{-1}), respectively, of annual primary production in these sectors.

The shelf exhibited the largest temporal increase in annual production of all the ecological provinces over the POI (R^2= 0.44, p=0.052), increasing each year by an average of 3.5 Tg C yr^{-1} (Fig. 11a). Although the 9-year trend was not statistically significant, increases in primary production were particularly dramatic for the last two years of the POI, exceeding 1998 levels by 70% and 63%, respectively, in 2005 and 2006. This increase was primarily due to a large and statistically significant (Table 1) increase in open water area in this province but also to a smaller (but not significant) increase in the daily area-normalized rate of production (Fig. 11a). Open water area in the shelf province increased from 0.66×10^6 km^2 in 1998 to 1.13×10^6 km^2 (in 2005) and 1.09×10^6 km^2 (in 2006), an increase of 71% and 64%, respectively. In contrast, the area-normalized production rate increased by 3.5% in 2005 and 24% in 2006, relative to the 1998 value. The area-normalized rate of production in the shelf province during the spring

bloom was the highest of all the other ecological provinces, averaging 790-1308 mg C m^{-2} d^{-1} (Fig. 10).

3.2.3.3. SMIZ

Total annual production in the SMIZ was the second largest of all the ecological provinces (Fig. 9a) and was comparable to that in the pelagic province, averaging 132 ± 6.0 Tg C yr^{-1} during the POI and representing 28-33% of the Arctic Ocean annual primary production. This was despite the fact that the SMIZ comprised on average only ~16% of the open water in the Arctic Ocean over a year. There was no significant interannual trend for total annual production in the SMIZ over the POI (R^2= 0.2, p=0.21, Table 3). The SMIZ province was particularly important in the Kara, Laptev and Siberian sectors, where it contributed >60% (>15 Tg C yr^{-1}) of annual primary production (Fig. 9). The SMIZ was the dominant province in the Chukchi, Beaufort, and Baffin sectors as well, accounting for 53% (14 Tg C yr^{-1}), 48% (10 Tg C yr^{-1}), and 35% (16 Tg C yr^{-1}) of sector-wide production, respectively.

The high total annual production in the SMIZ resulted from an area-normalized production rate that was higher than in any other ecological province, averaging 579± 42 mg C m^{-2} d^{-1} over the POI and reaching as high as 982-1174 mg C m^{-2} d^{-1} during the peak of the spring bloom (Fig. 10). The dominance of SMIZ persisted for most of the year, except during April-May when it was eclipsed by the daily production rate in the shelf province. The area-normalized production rate was highest in 2001 and 2006, averaging 650 and 606 mg C m^{-2} d^{-1}, respectively.

3.2.3.4. DMIZ

Annual production in the DMIZ was the lowest of all the ecological provinces (Fig. 9) and displayed no significant temporal trend during the POI (Table 3). With annual production rates averaging 47 ± 12 Tg C yr^{-1} (Fig. 9a), the DMIZ contributed just 9.6-13% of annual primary production in the Arctic Ocean. This low value was due more to a small amount of open water area in this province than to low area-normalized production rates, which were similar to those in

504 the pelagic province, averaging 347 ± 32 mg m^{-2} d^{-1} over the POI. Rates of area-normalized
505 production were highest in 2001 and 2006, exhibiting values of 377 and 379 mg m^{-2} d^{-1},
506 respectively (Fig. 10).
507 The DMIZ province was most productive in the Greenland sector (Fig. 9), contributing 18 Tg
508 C yr^{-1} or 14% of total annual production in this sector. Although the DMIZ accounts for a higher
509 proportion of annual production in the Beaufort (25%) and Baffin (21%) sectors, total DMIZ
510 production there (5 and 9 Tg C yr^{-1}, respectively) was considerably less than in the Greenland
511 sector.
512
513 **3.2.3.5. Total Shelves**
514 Despite accounting for only 30-40% of total open water area, the combined annual
515 production of the two provinces associated with the shallow waters of continental shelf, the shelf
516 and SMIZ provinces, contributed the majority of annual primary production in the Arctic (Fig.
517 9). Over the entire Arctic Ocean, the annual mean production in the waters of the shelf and
518 SMIZ combined (217 Tg C yr^{-1}) exceeded the production of the offshore waters of the pelagic
519 and the DMIZ provinces (201 Tg C yr^{-1}). Primary production on the continental shelves was
520 particularly important in the Chukchi, Siberian, Laptev, and Kara sectors, where the SMIZ+shelf
521 accounted for 90% or more of annual production.
522
523 **3.2.4. Controls of Primary Production**
524 In general, the spatial pattern of annual primary production (Fig. 12a) most closely mimics
525 that of Chl *a* over most of the Arctic Ocean (Fig. 12b). Of course the high correlation between
526 primary production and Chl *a* concentration (Fig. 13a) is to be expected, given that our algorithm
527 computes primary production from Chl *a* and an estimate of the phytoplankton growth rate (Eq.
528 2). While SST also plays an important role, the large amount of spatial and temporal variability
529 exhibited by Chl *a*, which can range over four orders of magnitude, far outweighs the relatively
530 smaller variability characteristic of SST. For example, primary production anomalies (Fig. 14),

531 calculated as the difference between the annual mean for a single year and the nine-year mean
532 (Fig. 12a), are largest (±80 g C m^{-2} yr^{-1}) in waters with high Chl *a* variability (Fig. 15).
533 Because phytoplankton blooms require ice-free surface waters in order to obtain sufficient
534 light for net growth, primary production also is positively correlated with open water area in
535 most sectors of the Arctic Ocean (Fig. 13b). The higher rates of primary production in the Arctic
536 in recent years are reflected in large and widespread positive primary production anomalies,
537 particularly in 2005 and 2006 (Fig. 14), that correspond to strong positive open water anomalies
538 (Fig. 16). In 2006, annual primary production was >60 g C m^{-2} yr^{-1} higher than the 9-year
539 average (Fig. 12a) in some parts of the Barents, Kara, and Greenland sectors. While
540 anomalously high rates of production in 2005 and 2006 were due in part to unusually high Chl *a*
541 concentrations (Fig. 15), open water conditions in some regions persisted for >150 days longer
542 than average (Fig. 16), greatly extended the length of the phytoplankton growing season. In the
543 Siberian sector, where open water area increased significantly during the POI, the changes in
544 production also were positive, although modest (20-40 g C m^{-2} yr^{-1}), especially since 2002. This
545 increase resulted from both higher Chl *a* concentrations and open water area in these waters after
546 2003. The negative primary production anomalies (<-60 g C m^{-2} yr^{-1}) in the Barents and Kara
547 sectors in 2003 were mainly due to anomalously low Chl *a* concentrations, since open water area
548 in these regions differed little from other years.
549 Primary production was positively correlated with SST (Fig. 13c) in all sectors except the
550 Greenland. The positive correlation of SST with primary production is due both to direct effects
551 of SST on phytoplankton growth rates (Eq. 2) and indirect effects of SST on surface water
552 stratification, impacting both light and nutrient availability. It is interesting to note that the
553 correlation between SST and annual primary production (Fig. 13c) is spatially similar to the
554 correlation between open water area and annual primary production (Fig. 13b), indicating that
555 the correlation between the SST and open water area is also high.
556

4. Discussion

4.1. Comparison with Previous Results

Unfortunately, there are very few historical estimates of pan-Arctic primary production with which to compare our results. *Subba Rao and Platt* [1984] estimated that the annual rate of Arctic-wide primary production for all waters north of 65°N was 206 Tg C yr^{-1}, approximately half the mean value estimated here (419 Tg C yr^{-1}). Because the study region in *Subba Rao and Platt* [1984] was slightly larger area than that used here, the primary reason for the discrepancy between the two values is that their estimate of mean area-normalized production for the Arctic (9-27 g C m^{-2} yr^{-1}) was considerably lower than ours (44 g C m^{-2} yr^{-1}). However, our value is in much better agreement with the much more recent pan-Arctic productivity estimate of 329 Tg C yr^{-1} made by *Sakshaug* [2003], which was based on a compilation of both historical measurements and model results. The computed annual primary production in the early years of our study is within 10% of the estimate of *Sakshaug* [2003]. This early period should bear a greater similarity to the historical observations compiled by *Sakshaug* [2003], which were made prior to the rapid increase in open water area observed recently. In later years (e.g., 2006), our estimate of production is 50% higher than that of *Sakshaug* [2003], due mostly to the dramatic increases in open water area but also to the slight increase in daily area-normalized production rates.

Annual rates of primary production computed here are likely to be underestimates of actual rates because, due to insufficient spatial resolution of satellite data, we are unable to quantify primary production in the leads and melt ponds within the Arctic sea ice zone that are known sinks for atmospheric CO_2 [*Semiletov et al.,* 2004]. Furthermore, the primary production algorithm does not account for production by phytoplankton growing under sea ice and by sea ice algae, although this is likely to represent only a small fraction of total Arctic primary production. Most importantly, calculated rates of primary production in the summer may be low because of the subsurface chlorophyll maximum (SCM) that occasionally develops offshore and is unresolved by SeaWiFS [*Falk-Peterson et al*., 2000; *Hill and Cota*, 2005; *Matrai et al*., 2007].

584 In some areas, productivity is highest at the ocean surface despite the presence of a SCM [e.g.
585 *Matrai et al*., 2007], suggesting that these SCMs were the result of an increase in phytoplankton
586 Chl *a* per cell with depth, rather than an actual subsurface peak in phytoplankton abundance. In
587 these waters, our algorithm should still work quite well. However, in those situations where the
588 depth of the SCM corresponds to the depth of the productivity peak [e.g. *Hill and Cota*, 2005],
589 depth-integrated water column production calculated by our algorithm is well below the *in situ*
590 estimate. For example, *Hill and Cota* [2005] observed numerous stations with a SCM in the
591 western Arctic. Surface Chl *a* at these stations averaged 0.4 mg m^{-3}, while the Chl *a*
592 concentration at the depth of the SCM averaged 2.5 mg m^{-3}. The depth-integrated primary
593 production for these stations averaged approximately 600 mg C m^{-2} d^{-1}, well above the range of
594 values produced by our algorithm for a surface Chl *a* concentration of 0.4 mg m^{-3} (Fig. 2b). The
595 prevalence of subsurface productivity maxima missed by SeaWiFS and their impact on annual
596 primary production estimates is unclear. Approximately 25% of the July-August stations shown
597 in Fig. 2b exhibited a significant subsurface productivity maximum that was not accounted for
598 by our algorithm. Given that July and August account for approximately 40% of annual primary
599 production (Fig. 7d), if our algorithm underestimated primary production over 25% of the Arctic
600 Ocean during these two months by as much as a factor of two, then the actual annual production
601 would be only 10% higher than we have estimated here.
602
603 **4.2. Temporal Changes in Primary Production**
604 Between 1998 and 2006, annual primary production in the Arctic Ocean increased by ~30%,
605 in sharp contrast to lower latitudes where primary production appears to have declined in recent
606 years [*Behrenfeld et al.,* 2006]. Changes in primary production in the Arctic also differed
607 markedly from trends observed in the Southern Ocean, where rates of annual production between
608 1997 and 2006 were ~5-fold higher than those estimated here, but with much less interannual
609 variability (11% versus 26% for the Arctic) and no significant temporal trend.

610 However, the change in annual primary production in the Arctic between 1998 and 2006 was
611 not monotonic (Fig. 8a), increasing in the early years of the POI (1998 to 2001), decreasing
612 thereafter until 2003, and then rising again to the maximum value attained during the POI in
613 2006 (483 Tg C yr^{-1}). Because of this irregular temporal pattern, the secular trend in annual
614 primary production was not statistically significant (R^2=0.4, p=0.07). In contrast, the amount of
615 open water area, which is a major factor controlling annual primary production, did exhibit a
616 statistically significant increase between 1998 and 2006 (Fig. 3a). This difference suggests that
617 the temporal trends observed in primary production were driven in large part by interannual
618 changes in the rate of area-normalized production, rather than by changes in sea ice extent. For
619 example, the local maximum in annual primary production in 2001 was the result of both higher
620 than normal phytoplankton biomass and higher area-normalized rates of production during the
621 late summer bloom of that year, despite open water area being relatively low (Fig. 3a). The
622 cause for this increase can clearly be seen by closer inspection of the primary production
623 anomaly in 2001 (Fig. 14), which shows that elevated production in the Barents and Kara sectors
624 coincided with a highly positive Chl *a* anomaly in these regions (Fig. 15), but with no
625 discernable changes in the open water area (Fig. 16) or SST (Fig. 17). Similarly, the drop in
626 annual production between 2001 and 2003, despite a slight increase in open water area, was
627 closely tied to a coincident drop in area-normalized production in all four of the ecological
628 provinces in the Arctic Ocean (Fig. 11). Thus, changes in total production in the Arctic were not
629 simply a consequence of increased open water area in recent years; changes in phytoplankton
630 biomass and area-normalized production also played important roles. This was especially true in
631 2005 and 2006 when both the area-normalized rate of production and open water area were at or
632 near their nine-year highs, elevating 2006 to the most productive year of the POI.
633 Although the precise cause of the observed interannual variation in area-normalized
634 production is not clear, changes taking place in the Greenland Sea, particularly from 2004-2006,
635 may provide some clues. Over most of the Arctic, we observed a strong positive correlation
636 between annual mean SST and annual primary production (Fig. 13c). The major exception to

637 this pattern is found in those parts of the Greenland Sea that remain ice-free all year (red areas in
638 Fig. 12c). In these waters, positive SST anomalies (Fig. 17) coincided with negative primary
639 production anomalies (Fig. 14), resulting in an atypical negative correlation between SST and
640 annual primary production (Fig. 13c). The temperature of these waters is known to be especially
641 sensitive to the phase of the Arctic Oscillation (AO) [*Wanner et al.*, 2001]. As the AO becomes
642 more positive, westerly winds strengthen, northward advection of North Atlantic waters
643 increases, and waters in the western Greenland Sea cool [*Thompson and Wallace*, 1998]. As can
644 be seen in our study, a cooler Greenland Sea is associated with enhanced Chl *a* concentrations in
645 these waters and positive annual primary production anomalies. This pattern is particularly
646 evident from 2004 through 2006, when cooling of the open waters of the Greenland Sea (Fig. 17)
647 was associated with a marked increase in both Chl *a* (Fig. 16) and primary production (Fig. 14).
648 Although the mechanism behind the elevated production in a cooler Greenland Sea is not
649 presently known, the increased northward advection of North Atlantic water during positive
650 phases of the AO may enhance the flux nutrients into the Greenland Sea that stimulate the
651 growth of phytoplankton and increase annual primary productivity.
652 It should be noted, however, that the temporal pattern of annual pan-Arctic primary
653 production was not well correlated with the AO index (data from the NOAA climate monitoring
654 center, http://www.cpc.ncep.noaa.gov/products/precip/CWlink/daily_ao_index/ao_index.html),
655 averaged either annually (R^2=0.016, p=0.74) or only over the more critical winter months
656 (November-April, R^2=0.013, p=0.77). However, the AO is most highly correlated with annual
657 primary production in the Greenland Sea, by far the most productive sector of the Arctic Ocean
658 (Fig. 9), although even there it explains only 29% of the interannual variability (p=0.12) between
659 1998 and 2006. This lends support to the notion that increased advection of waters into the
660 Greenland Sea during a positive phase of the AO could play an important role in enhancing
661 phytoplankton productivity. It must be remembered, however, that the AO is complex and does
662 not actually exist in two quasi-stable states (positive or negative), as was suggested by the simple
663 description given above. Instead, the AO is highly dynamic and can vary markedly on monthly

time scales. Thus, it is not surprising that the correlation between annual primary production and the AO is relatively weak, even in the Greenland Sea where its impacts are expected to be most apparent.

4.3. Recent Loss of Sea Ice

The results presented in this study show that during 1998-2006, the loss of sea ice (and increase in open water area) was not uniform across the Arctic, being more pronounced in some geographic sectors than in others. Open water area increased most rapidly in the Barents and Kara sectors, and most significantly in the Siberian sector. The observed decrease in sea ice in these sectors is consistent with the previously documented decreasing trend in ice thickness between 1987 and 1999 by *Rothrock et al.* [2003]. The dramatic loss of sea ice in the Siberian sector is particularly alarming because model results demonstrate that changes in the Siberian Sea can be a precursor to basin-wide changes in sea ice thickness [*Rothrock et al.*, 2003; *Ukita et al*., 2007]. Our study shows that the rate of loss of sea ice in these waters has been accelerating in recent years, particularly since 2003.

The accelerated changes of sea ice extent and thickness in the Arctic are due to multiple factors. Foremost is the loss of ice due to wind stress changes that increase the advection of sea ice out of the Arctic [*Zhang et al.,* 2000; *Holloway and Sou* 2002]. This impact can be amplified by increased melting and a longer melt-season, resulting in a positive feedback on sea ice loss [*Smith et al.*, 1998; *Laxon et al.*, 2003]. The rate of sea ice melt also may be accelerated by the observed increase in water temperature in recent years. This temperature increase has been attributed to a combination of warmer Pacific waters entering through the Bering Strait [*Fukasawa et. al*., 2004; *Shimada et al.,* 2006] and a rise in downward longwave radiation [*Francis and Hunter*, 2006] resulting from increase in liquid-water clouds relative to ice clouds [*Zuidema et al*., 2005; *Francis and Hunter*, 2006]. Consistent with this viewpoint, *Serreze et. al.*[2003] suggested that the recent changes in Arctic sea ice cover, particularly the low sea ice extent in 2002, were due to increased advection of heat into the Arctic Ocean during spring,

coupled with high temperature and low pressure in summer that was affected by the cyclogenesis along northeastern Eurasia. In contrast, *Rigor et al*. [2002] and *Rigor and Wallace* [2004] argue that anomalous changes in sea ice are due to winter wind anomalies associated with the high-index AO conditions that increase the advection of ice away from the Eurasian and Alaskan coasts. Regardless of the relative importance of meteorological conditions in the winter and spring, losses of Arctic ice have been extensive in recent years, exemplified by the dramatic 30% decrease between 2006 and 2007 in the extent of perennial sea ice during the summer [*Comiso et al*, 2008].

4.4. Other Environmental Changes in the Arctic

Primary production in the Arctic is likely to vary in response to changes in a number of other environmental factors that influence the onset and development of phytoplankton blooms, including PAR at the upper ocean surface, nutrient inventories, and freshwater content. For example, mean Arctic-wide PAR exhibited a slow but steady decrease during the POI, dropping each year by an average of 0.7 μEin m^{-2} s^{-1} (R^2=0.74). PAR was highest in 1999 (annual mean of 201 μEin m^{-2} s^{-1}) and lowest in 2006 (annual mean of 195 μEin m^{-2} s^{-1}). Using our primary production algorithm, we calculate that the observed 3% decrease in PAR between 1999 and 2006 should translate into in a 1% decrease in annual primary production.

More importantly, there has been a significant rise in freshwater content in the Arctic due to melting of sea ice and glaciers, excess precipitation, and increasing river discharge [*Peterson et. al.,* 2002]. The rise in river discharge is due primarily to increased runoff from Asian rivers, which currently adds 2560 km^3 of freshwater to the Arctic Ocean each year, an increase of 5% over the mean from the previous 20 years [*Richter-Menge et. al.,* 2006]. Discharge from the Yukon and Mackenzie rivers in recent years also was higher than normal [*Richter-Menge et. al.*, 2006], most likely due to an increase in net excess precipitation over evaporation (P-E) at high latitudes [*Peterson et al.,* 2002]. Enhanced melting of glaciers [*Dyurgherov and Carter*, 2004] and the Greenland ice sheet [*Box et al*., 2004] further contributed to the recent increase in

718 freshwater content of the Arctic. Finally, the contribution of freshwater from melting sea ice in
719 the Arctic increased from 8000 km^3 in 1980 to 17,000 km^3 in 1997 [*Peterson et al.,* 2006].
720 These changes in Arctic freshwater input, especially from river runoff (which also contributes
721 substantial amounts of sediment and organic matter), alter the availability of both nutrients and
722 light necessary for phytoplankton growth. Increasing freshwater content intensifies surface
723 stratification, thereby decreasing the thickness of the upper mixed layer, increasing light
724 availability and partially offsetting the drop in irradiance due to increased turbidity and decreases
725 in incident PAR. On the other hand, increased stratification would likely reduce the supply of
726 nutrients from the deeper waters beneath the mixed layer, decreasing phytoplankton growth and
727 productivity.
728 While increasing air temperature appears to have governed the processes of excess river
729 discharge and accelerated sea ice melt in recent years, the P-E anomaly seems to be more closely
730 tied to the changes in the AO [*Peterson et al.,* 2006]. *Steele and Ermold* [2004] report
731 considerable freshening of the western Siberian shelf sea (White Sea and Kara Sea) and
732 salinification of the eastern Siberian shelf seas. Fresh water tends to accumulate in the Arctic
733 Ocean during the negative phase of the AO and subsequently exits to the North Atlantic during
734 the positive AO phase [*Dickson,* 1999]. However, the poor correlation we report between the
735 AO index and both phytoplankton biomass and primary production in the Arctic suggests that
736 these oceanographic manifestations of the AO may be very localized or may operate on
737 timescales or at times of year that reduce their impact on phytoplankton productivity in the
738 Arctic. The AO seems to exert its greatest influence during the coldest part of the year
739 (November-April), when low light conditions preclude phytoplankton growth. The extent to
740 which stratification intensified by a negative AO persists into the spring and summer may
741 ultimately determine its impact on rates of primary production.
742

743 **4.5. Future Changes in Arctic Ocean Phytoplankton Productivity**

744 The increase in the flux of CO_2 from the atmosphere into the Arctic Ocean has tripled over
745 the last 3 decades (from 24 to 66 Tg C yr^{-1}) [*Bates et al.,* 2006]. This increase is attributed to the
746 recent loss of sea ice that facilitated both increased primary production and sea-air CO_2
747 exchange. The recent increase in primary production reported here should further enhance this
748 exchange, due to the reduction in surface water pCO_2 during the conversion of inorganic CO_2 to
749 organic carbon by phytoplankton that eventually sinks below the thermocline. Although it has
750 been calculated that outgassing of CO_2 will increase by 8 g C m^{-2} yr^{-1} for every 1ºC increase in
751 sea surface temperature [*Anderson and Kaltin,* 2001], the biologically-mediated decrease in
752 surface pCO_2 should partially offset the increased outgassing of CO_2 expected as Arctic surface
753 waters warm in upcoming years. In fact, it has been suggested that when anticipated changes in
754 CO_2 solubility (due to changes in both temperature and salinity) and phytoplankton production
755 are taken into account, the potential for the Arctic Ocean to act as a sink for atmospheric CO_2
756 will increase in the future [*Anderson and Kaltin,* 2001]. However, longer-term observations are
757 required to understand the extent to which primary production will be either intensified or
758 weakened by the many concurrent environmental changes ongoing in the Arctic Ocean (e.g.,
759 declines in sea ice cover, increased SST, increased freshwater fluxes, changes in nutrient and
760 light availability). In addition, although our study quantifies large-scale changes in the primary
761 production of northern polar seas, it is unable to address any ongoing taxonomic changes within
762 the phytoplankton community within the Arctic Ocean [*Booth and Horner*, 1997] as a
763 consequence of observed environmental changes. Finally, further studies are required to
764 quantify the extent to which the negative feedback between losses of sea ice and increased
765 biological CO_2 uptake in the Arctic (which would reduce atmospheric warming) will be
766 countered by the increased CO_2 outgassing resulting from surface ocean warming due to reduced
767 sea ice albedo [*Morales Maqueda et al.*, 1999]. This understanding is particularly critical given
768 the unprecedented acceleration of sea ice loss observed in the Arctic in recent years.
769

Acknowledgements

This research was supported by a NASA Earth Systems Science fellowship to S. Pabi (ESSF/04-0000-0293) and NASA grant NNG05GC92G to K. Arrigo. We would like to thank Jean-Eric Tremblay and the SBI investigators who made their data available for algorithm validation. We would like to thank Lindsey Kropuenske for comments on earlier version of this manuscript.

References

Arctic Climate Impact Assessment (ACIA) (2005), Cambridge University Press, Cambridge, United Kingdom and New York, NY, USA.

Anderson, L. G., and S. Kaltin (2001), Carbon fluxes in the Arctic Ocean - potential impact by climate change, *Polar Res., 20*(2), 225-232.

Arrigo, K. R., and C. W. Sullivan (1994), A high resolution bio-optical model of microalgal growth: Tests using sea ice algal community time-series data, *Limnol. Oceanogr., 39*(3), 609-631.

Arrigo, K. R., D. Worthen, A. Schnell, and M. P. Lizotte (1998), Primary production in Southern Ocean waters, *J. Geophys. Res., 103*, 15587-15600.

Arrigo, K. R., G. L. van Dijken, and S. Bushinsky (2008), Primary production in the Southern Ocean, 1997-2006, *J. Geophys. Res*.

Bates, N. R., S. B. Moran, D. A. Hansell, and J. T. Mathis (2006), An increasing CO_2 sink in the Arctic Ocean due to sea ice loss, *Geophys. Res. Lett., 33*(23), L23609.

Behrenfeld, M., and P. Falkowski (1997), Photosynthetic rates derived from satellite-based chlorophyll concentration, *Limnol. Oceanogr., 42*(1), 1-20.

Behrenfeld, M. J., R. T. O'Malley, D.A. Siegel, C. R. McClain, J. L. Sarmiento, G. C. Feldman, A. J. Milligan, P. G. Falkowski, R. M. Letelier, and E. S. Boss (2006), Climate-driven trends in contemporary ocean productivity, *Nature*, *444*(7120), 752-755.

Boetius, A. and E. Damm (1998), Benthic oxygen uptake, hydrolytic potentials and microbial biomass at the Arctic continental slope, *Deep-Sea Res., Part I, 45*(2-3), 239-275.

797 Box, J. E., D. H. Bromwich, and Le-Sheng Bai (2004), Greenland ice sheet surface mass balance
798 1991-2000: application of Polar MM5 mesoscale model and in situ data, *J. Geophys. Res.,*
799 *109*, D16105, doi:10.1029/2003JD004451.
800 Buck, K. R., T. G. Nielsen, B. W. Hansen, D. Gastrup-Hansen, and H. A. Thomsen (1998),
801 Infiltration phyto- and protozooplankton assemblages in the annual sea ice of Disko Island,
802 West Greenland, spring 1996, *Polar Biol.,* 20(6), 377-381.
803 Carmack, E. C., K. Aagaard, J. H. Swift, R. W. MacDonald, F. A. McLaughlin, E. P. Jones, R.
804 G. Perkin, J. N. Smith, K. M. Ellis, and L. R. Killius (1997), Changes in temperature and
805 tracer distributions within the Arctic Ocean: results from the 1994 Arctic Ocean Section,
806 *Deep-Sea Res., Part II, 44*(8), 1487-1502.
807 Carmack, E. C., and R. W. Macdonald (2002), Oceanography of the Canadian shelf of the
808 Beaufort Sea: A setting for marine life, *Arctic, 55*, 29-45.
809 Cavalieri, D. J., C. L. Parkinson, and K. Y. Vinnikov (2003), 30-year satellite record reveals
810 contrasting Arctic and Antarctic decadal sea ice variability, *Geophys. Res. Lett., 30*(18),
811 CRY4-1.
812 Chapman, W. L., and J.E.Walsh (2003), Observed climate change in the Arctic, updated from
813 Chapman and Walsh, 1993: Recent variations of sea ice and air temperatures in high
814 latitudes, *Bull. Am. Met. Soc., 74*(1), 33-47.
815 Codispoti, L. A. (1979), Arctic Ocean processes in relation to the dissolved silicon content of the
816 Atlantic, *Mar. Sci. Commun., 5*(6), 361-381.
817 Comiso J. C., C. L. Parkinson, R. Gersten, L. Stock (2008), Accelerated decline in the Arctic sea
818 ice cover, *Geophys. Res. Lett*., *35*, L01703, doi:10.1029/2007GL031972.
819 Dickson, B. (1999), Oceanography - All change in the Arctic, *Nature, 397*(6718), 389-391.
820 Dobson, F. W., and Smith, S.D. (1988), Bulk models of solar radiation at sea, Quarterly Journal
821 of the Royal Meteorological Society, *114*, 165-182.
822 Dyurgerov, M. B., and C. L. Carter (2004), Observational evidence of increases in freshwater
823 inflow to the Arctic Ocean, *Arctic Antarctic and Alpine Research, 36*(1), 117-122.

824 Eppley, R. W. (1972), Temperature and phytoplankton growth in the sea, *Fishery Bull.*
825 (Washington D C), *70*(4), 1063-1085.
826 Falk-Petersen, S., H. Hop, W. Budgell, E. Hegseth, R. Korsnes, T. Loyning, J. Orbaek, T.
827 Kawamura, and K. Shirasawa (2000), Physical and ecological processes in the marginal ice
828 zone of the northern Barents Sea during the summer melt period, *J. Mar. Sys., 27*(1-3), 131-
829 159.
830 Francis, J. A. and E. Hunter (2006), New insight into the disappearing Arctic sea ice, *Eos Trans.*
831 *AGU*, 87(46), 509.
832 Fukasawa, M., H. Freeland, R. Perkin, T. Watanabe, H. Uchida, and A. Nishina (2004), Bottom
833 water warming in the North Pacific Ocean, *Nature, 427*(6977), 825-7.
834 Gosselin, M., M. Levasseur, P. A. Wheeler, R. A. Horner, and B. C. Booth (1997), New
835 measurements of phytoplankton and ice algal production in the Arctic Ocean, *Deep-Sea*
836 *Res., Part II, 44*(8), 1623-1644.
837 Gregg, W. W., and K. L. Carder (1990), A simple spectral solar irradiance model for cloudless
838 maritime atmospheres, *Limnol. Oceanogr., 35*(8), 1657-1675.
839 Harrison, W., and G. Cota (1991), Primary production in polar waters - relation to nutrient
840 availability, *Polar Res., 10*(1), 87-104.
841 Hill, V., and G. Cota (2005), Spatial patterns of primary production on the shelf, slope and basin
842 of the Western Arctic in 2002, *Deep-Sea Res., Part II, 52*(24), 3344-54.
843 Holloway, G., and T. Sou (2002), Has Arctic sea ice rapidly thinned? *J. Climate, 15*(13), 1691-
844 701.
845 IPCC. Intergovernmental Panel on Climate Change - 4th Assessment Report (2006),
846 http://www.ipcc.ch/activity/ar.htm
847 Jakobsson, M., A. Grantz, Y. Kristoffersen, and R. Macnab (2003), Physiographic provinces of
848 the Arctic Ocean seafloor, *Bull. Geol. Soc. Am., 115*(12), 1443-1455.
849 Johannessen, O., E. Shalina, and M. Miles (1999), Satellite evidence for an Arctic sea ice cover
850 in transformation, *Science, 2886*(5446), 1937-9.

851 Kirk, J. T. O. (1983) *Light and Photosynthesis in the Aquatic Ecosystems* Cambridge University
852 Press, Cambridge.
853 Laxon, S., N. Peacock, and D. Smith (2003), High interannual variability of sea ice thickness in
854 the Arctic region, *Nature, 425*(6961), 947-50.
855 Legendre, L., S. F. Ackley, G. S. Dieckmann, B. Gullicksen, R. Horner, T. Hoshiai, I. A.
856 Melnikov, W. S. Reeburgh, M. Spindler and C. W. Sullivan (1992), Ecology of sea ice
857 biota: 2. Global significance. *Polar Biol.*, *12*, 429-444.
858 Levi, B. G. (2000), The decreasing Arctic ice cover, *Physics Today, 53*(1), 19-20.
859 Macdonald, R. (1996), Oceanography - Awakenings in the Arctic, *Nature, 380*(6572), 286-287.
860 Macdonald, R. W., S. M. Solomon, R. E. Cranston, H. E. Welch, M. B. Yunker, and C. Gobeil
861 (1998), A sediment and organic carbon budget for the Canadian Beaufort shelf, *Mar. Geol.,*
862 *144*(4), 255-273.
863 Markus, T., and B. A. Burns (1995), A method to estimate subpixel-scale coastal polynyas with
864 satellite passive microwave data, *J. Geophys. Res., 100*, 4473-4487.
865 Maslowski, W., D. Marble, W. Walczowski, U. Schauer, J. L. Clement, and A. J. Semtner
866 (2004), On climatological mass, heat, and salt transports through the Barents Sea and Fram
867 Strait from a pan-Arctic coupled ice-ocean model simulation, *J. Geophys. Res., 109*(C3),
868 C03032, doi:10.1029/2001JC001039
869 Matrai, P, M. Vernet and P. Wassmann (2007), Relating temporal and spatial patterns of DMSP
870 in the Barents Sea to phytoplankton biomass and productivity. *J. Mar. Sys*., *67*, 83-101.
871 Matsuoka, A., S. Saitoh, and K. Shimada (2005), A new approach for ocean color algorithm in
872 Case 2 water using bio-optical field measurements in the Western Arctic Ocean,
873 *Proceedings of SPIE - The International Society for Optical Engineering, 5977*.
874 Menard, H. W., and S. M. Smith (1966), Hypsometry of ocean basin provinces, *J. Geophys. Res.,*
875 *71*(18), 4305-4325.
876 McLaughlin, F., K. Shimada, E. Carmack, M. Itoh, and S. Nishino (2002), The hydrography of
877 the southern Canada Basin, *Polar Biol., 28*(3), 182-189, doi: 10.1007/s00300-004-0701-6.

878 Morales-Maqueda, M. A., A. J. Willmott, and M. S. Darby (1999), A numerical model for
879 interdecadal variability of sea ice cover in the Greenland-Iceland-Norwegian Sea, *Climate*
880 *Dynamics, 15*(2), 89-113.
881 Morel, A. (1978), Available, usable, and stored radiant energy in relation to marine
882 photosynthesis, *Deep-Sea Res., 25*(8), 673-88.
883 Morel, A. (1987), Chlorophyll-specific scattering coefficient of phytoplankton a simplified
884 theoretical approach, *Deep-Sea Res., Part A, 34*(7), 1093-1106.
885 Morel, A. (1991), Light and marine photosynthesis: a spectral model with geochemical and
886 climatological implications. *Prog. Oceanogr., 26*(3), 263-306.
887 Niebauer, H., A. V, and S. Henrichs (1990), Physical and biological oceanographic interaction in
888 the spring bloom at the Bering Sea marginal ice edge zone, *J. Geophys. Res., 95*(C12),
889 22229-22241.
890 NSIDC, National Snow and Ice Data Center (2007),
891 http://nsidc.org/news/press/2007_seaiceminimum/20071001_pressrelease.html.
892 O'Reilly, J., S. Maritorena, B. Mitchell, D. Siegel, K. Carder, S. Garver, M. Kahru, and C.
893 McClain (1998), Ocean color chlorophyll algorithms for SeaWiFS. *J. Geophys. Res.,*
894 *103*(C11), 24937-53.
895 Parkinson, C. L. (2000), Variability of Arctic sea ice: The view from space, and 18-year record.
896 *Arctic, 53*, 341-358.
897 Peterson, B. J., R. M. Holmes, J. W. McClelland, C. J. Vorosmarty, R. B. Lammers, A. I.
898 Shiklomanov, I. A. Shiklomanov, and S. Rahmstorf (2002), Increasing river discharge to the
899 Arctic Ocean, *Science, 298*(5601), 2171-3.
900 Peterson, B. J., J. McClelland, R. Curry, R. M. Holmes, J. E. Walsh, and K. Aagaard (2006),
901 Trajectory shifts in the Arctic and subarctic freshwater cycle, *Science, 313*(5790), 1061-6.
902 Platt, T., W. G. Harrison, B. Irwin, E. P. Horne, and C. L. Gallegos (1982), Photosynthesis and
903 Photoadaptation of marine phytoplankton in the Arctic, *Deep Sea Res, 29*(10), 1159-1170.

Reynolds, R.W., N.A. Rayner, T.M. Smith, D.C. Stokes, and W. Wang (2002), An improved in situ and satellite SST analysis for climate. *J. Climate*, *15*, 1609-1625.

Richter-Menge et al., (2006). State of the Arctic Report, NOAA OAR Special Report, NOAA/OAR/PMEL, Seattle, WA, 36 pp.

Rigor, I. G., J. M. Wallace, and R. L. Colony (2002), Response of sea ice to the Arctic Oscillation, *J. Climate, 15*(18), 2648.

Rigor, I. G., and J. M. Wallace (2004), Variations in the age of Arctic sea ice and summer sea ice extent, *Geophys. Res. Lett., 31*(9), L09401 1-4.

Rothrock, D. A., Y. Yu, and G. A. Maykut (1999), Thinning of the Arctic sea ice cover, *Geophys. Res. Lett., 26*(23), 3469.

Rothrock, D. A., J. Zhang, and Y. Yu (2003), The arctic ice thickness anomaly of the 1990s: A consistent view from observations and models, *J. Geophys. Res., 108*, 28-1.

Sakshaug, E., K. Andresen, S. Myklestad, and Y. Olsen (1983), Nutrient status of phytoplankton communities in Norwegian waters (marine, brackish and fresh) as revealed by their chemical composition, *J. Plank. Res., 5*(2), 175-196.

Sakshaug, E. (2003), Primary and secondary production in the Arctic Seas, in *The organic carbon cycle in the Arctic Ocean.*edited by Stein R, Macdonald RW, pp. 57-81, Springer-Verlag, Berlin.

Serreze, M. C., J. A. Maslanik, T. A. Scambos, F. Fetterer, J. Stroeve, K. Knowles, C. Fowler, S. Drobot, R. G. Barry, and T. M. Haran (2003), A record minimum arctic sea ice extent and area in 2002, *Geophys. Res. Lett.*, *30*(3), 10-14.

Serreze, M. C., Holland, M. M., Stroeve, J (2007), Perspectives on the Arctic's shrinking sea-ice cover, *Science, 315*(5818), 1533-1536.

Shiklomanov, I. A. (2000), Appraisal and assessment of world water resources, *Water International, 25*(1), 11.

929 Shimada, K., T. Kamoshida, M. Itoh, S. Nishino, E. Carmack, F. McLaughlin, S. Zimmermann,
930 and A. Proshutinsky (2006), Pacific Ocean inflow: influence on catastrophic reduction of
931 sea ice cover in the Arctic Ocean, *Geophys. Res. Lett., 33*(8), 4.
932 Smith, D. M. (1998), Recent increase in the length of the melt season of perennial Arctic sea ice,
933 *Geophys. Res. Lett., 25*(5), 655-8.
934 Steele, M., and W. Ermold (2004), Salinity trends on the Siberian shelves, *Geophys. Res. Lett.,*
935 *31*(24), L24308.
936 Subba Rao, D. V. and T. Platt (1984), Primary productivity of Arctic waters, *Polar Biol.*, *3*, 191-
937 201.
938 Thompson, D. W. J., and J. M. Wallace (1998), Arctic Oscillation signature in the wintertime
939 geopotential height and temperature fields, *Geophys. Res. Lett., 25*(9), 1297-1300.
940 Tremblay, J. E., Y. Gratton, J. Fauchot, and N. M. Price (2002), Climatic and oceanic forcing of
941 new, net, and diatom production in the North Water, *Deep-Sea Res., Part II, 49*(22), 4927-
942 4946.
943 Ukita, J., M. Honda, H. Nakamura, Y. Tachibana, D. J. Cavalieri, C. L. Parkinson, H. Koide, and
944 K. Yamamoto (2007), Northern Hemisphere sea ice variability: lag structure and its
945 implications, *Tellus Series A-Dynamic Meteorology and Oceanography, 59*(2), 261-272.
946 Vedernikov V.I., D.,A.B., and A. I. Sudbin (1994), Primary production and chlorophyll in the
947 Kara Sea in September 1993, *Okeanologiya, 34*(5), 693-703.
948 Walsh, J. J., et al (2005), A numerical model of seasonal primary production within the
949 Chukchi/Beaufort seas, *Deep-Sea Res., Part II, 52*(24), 3541-76.
950 Wanner, H., S. Bronnimann, C. Casty, D. Gyalistras, J. Luterbacher, C. Schmutz, D. B.
951 Stephenson, and E. Xoplaki (2001), North Atlantic Oscillation - Concepts and studies,
952 *Surveys in Geophysics, 22*(4), 321-382.
953 Wang, J., and G. F. Cota (2003), Remote-sensing reflectance in the Beaufort and Chukchi seas:
954 Observations and models, *Applied Optics, 42*(15), 2754.

955 Wassmann, P., and D. Slagstad (1993), Seasonal and annual dynamics of particulate carbon flux
956 in the Barents Sea: A model approach, *Polar Biol., 13*(6), 363-372.
957 Zhang, J. L., D. Rothrock, and M. Steele (2000), Recent changes in Arctic sea ice: the interplay
958 between ice dynamics and thermodynamics, *J. Climate, 13*(17), 3099-3114.
959 Zuidema, P., E. R. Westwater, C. Fairall, and D. Hazen (2005), Ship-based liquid water path
960 estimates in marine stratocumulus, *J. Geophys. Res., 110*, D20206.
961

961 **Figure legends**

962 Figure 1. Map of the study area showing (a) bathymetry (in meters), the location of the Arctic
963 Circle (shown in black), and the distribution of the eight geographic sectors (map
964 adapted from the International Bathymetric Chart of the Arctic Ocean) and (b) an
965 example of the locations of the four ecological provinces (September 1998).

966 Figure 2. Plots of surface Chl *a* versus daily primary production estimated from our primary
967 production algorithm and measured *in situ* at discrete stations from the Chukchi and
968 Beaufort seas obtained during the Shelf Basin Interaction program during a) May-June
969 2002 and b) July-August 2002. Algorithm output used in this analysis was restricted
970 to those times and locations for which *in situ* data were available.

971 Figure 3. Open water area in the Arctic Ocean averaged over a) the entire year, b) the months of
972 May-June (time of the a spring bloom), and c) the months of August-September (time
973 of maximum open water). Also shown is the long-term trend in mean open water area.

974 Figure 4. Weekly changes in a) open water area and b) sea surface temperature during 1998-
975 2006.

976 Figure 5. Annual mean open water area in the Arctic Ocean for each ecological province and
977 geographical sector during 1998-2006.

978 Figure 6. Weekly changes in open water area in the four ecological provinces of the Arctic
979 Ocean during 1998-2006.

980 Figure 7. Weekly changes in a) mean surface Chl *a* concentration, b) mean daily
981 photosynthetically active radiation (PAR) incident at the sea surface, c) mean area-
982 normalized daily primary production, and d) annual primary production in the Arctic
983 Ocean during 1998-2006.

984 Figure 8. Total primary production computed for a) the entire year, b) the months of May-June,
985 and c) the months of August-September. Also shown is the long-term trend in primary
986 production.

Figure 9. Annual primary production in the Arctic Ocean for each ecological province and geographical sector during 1998-2006.

Figure 10. Weekly changes in daily area-normalized primary production in each ecological province of the Arctic Ocean during 1998-2006.

Figure 11. Total annual primary production (grey columns, Tg C yr^{-1}), annual mean open water area and annual mean area-normalized primary production in the a) shelf, b) SMIZ, c) DMIZ, and d) pelagic provinces of the Arctic Ocean during 1998-2006.

Figure 12. Climatologies (1998-2006) for a) annual primary production, b) annual mean surface Chl *a*, c) annual mean open water (number of ice-free days per year), and d) annual mean sea surface temperature.

Figure 13. Maps of the correlation coefficient for the regression of annual mean primary production against a) annual mean surface Chl *a*, b) annual mean open water area (only in regions where open water is present for ≤350 days), and c) annual mean sea surface temperature for the nine years of our study. Only pixel locations where data are available for all nine years are shown in color.

Figure 14. Anomaly maps of annual primary production for each of the nine years of this study. Colors represent change from the climatological mean shown in Fig. 14a.

Figure 15. Anomaly maps of surface Chl *a* for each of the nine years of this study. Colors represent change from the climatological mean shown in Fig. 14b.

Figure 16. Anomaly maps of open water area for each of the nine years of our study. Colors represent change from the climatological mean shown in Fig. 14c.

Figure 17. Anomaly maps of sea surface temperature for each of the nine years of our study. Colors represent change from the climatological mean shown in Fig. 14d.

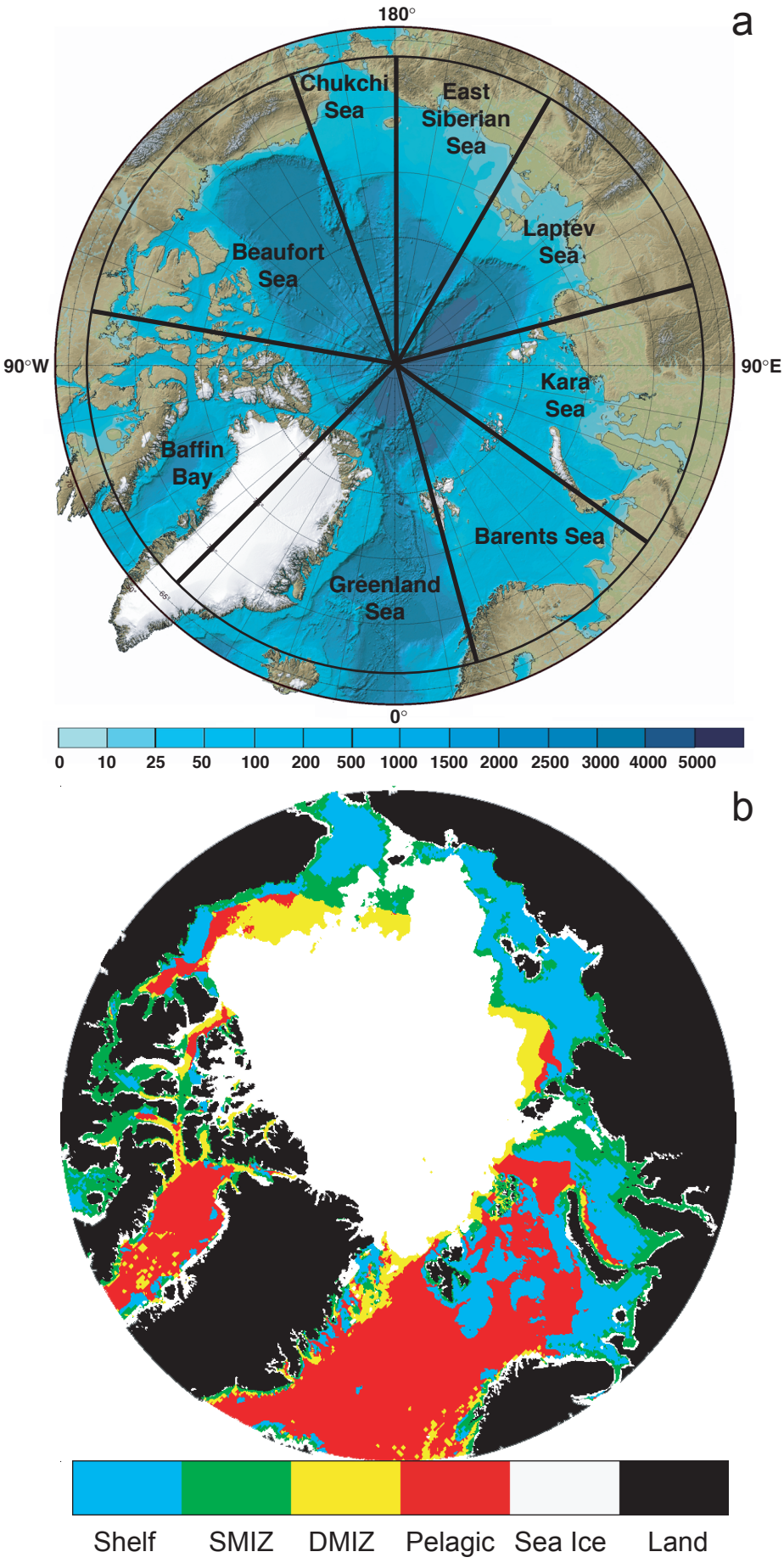
a
180°
90°W
90°E
0°
Chukchi Sea
East Siberian Sea
Laptev Sea
Beaufort Sea
Kara Sea
Baffin Bay
Barents Sea
Greenland Sea
0 10 25 50 100 200 500 1000 1500 2000 2500 3000 4000 5000
b
Shelf
SMIZ
DMIZ
Pelagic
Sea Ice
Land

Figure 1

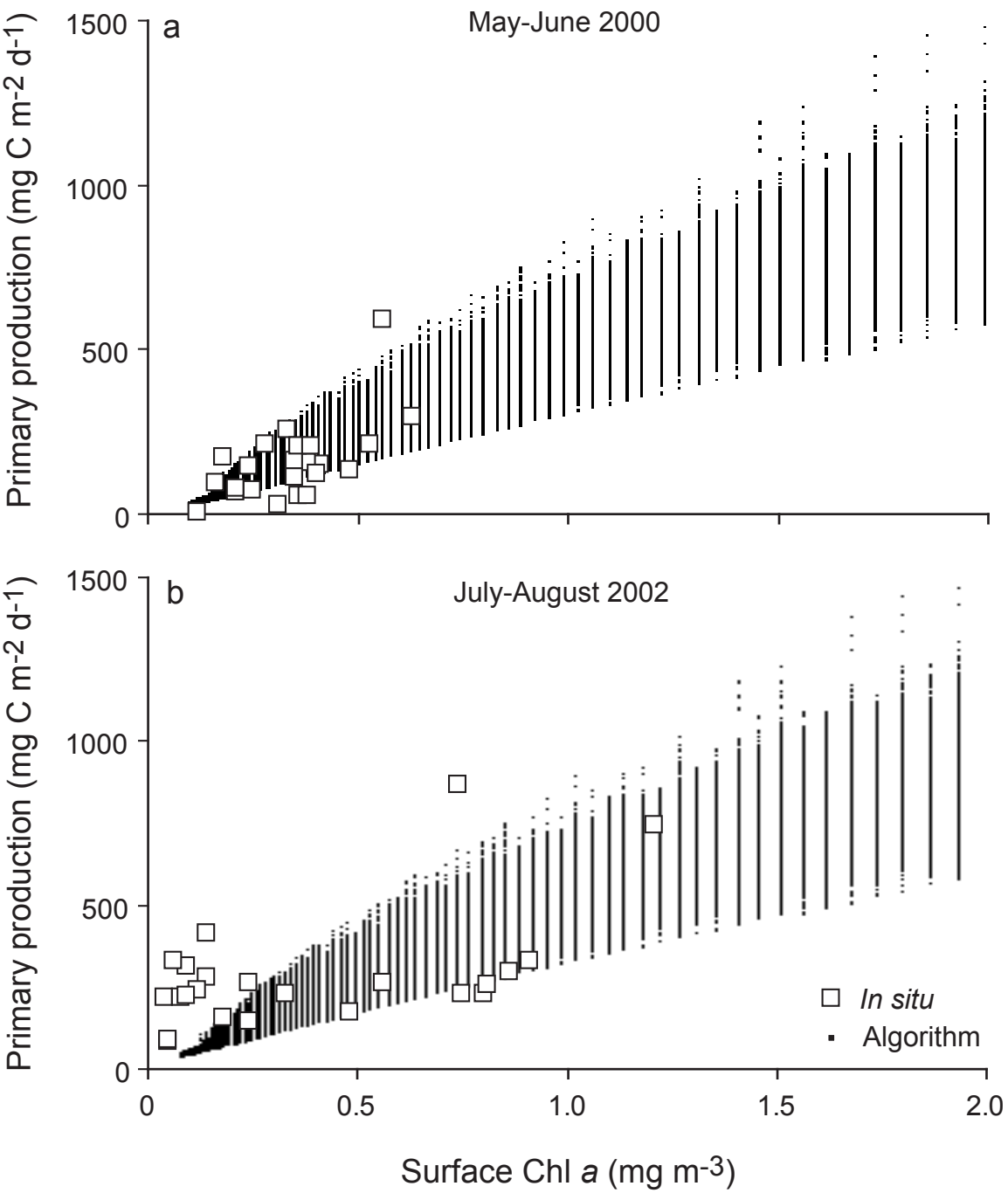
a
May-June 2000
b
July-August 2002
Primary production (mg C m-2 d-1)
1500
1000
500
0
0
0.5
1.0
1.5
2.0
In situ
Algorithm
Surface Chl a (mg m-3)

Figure 2

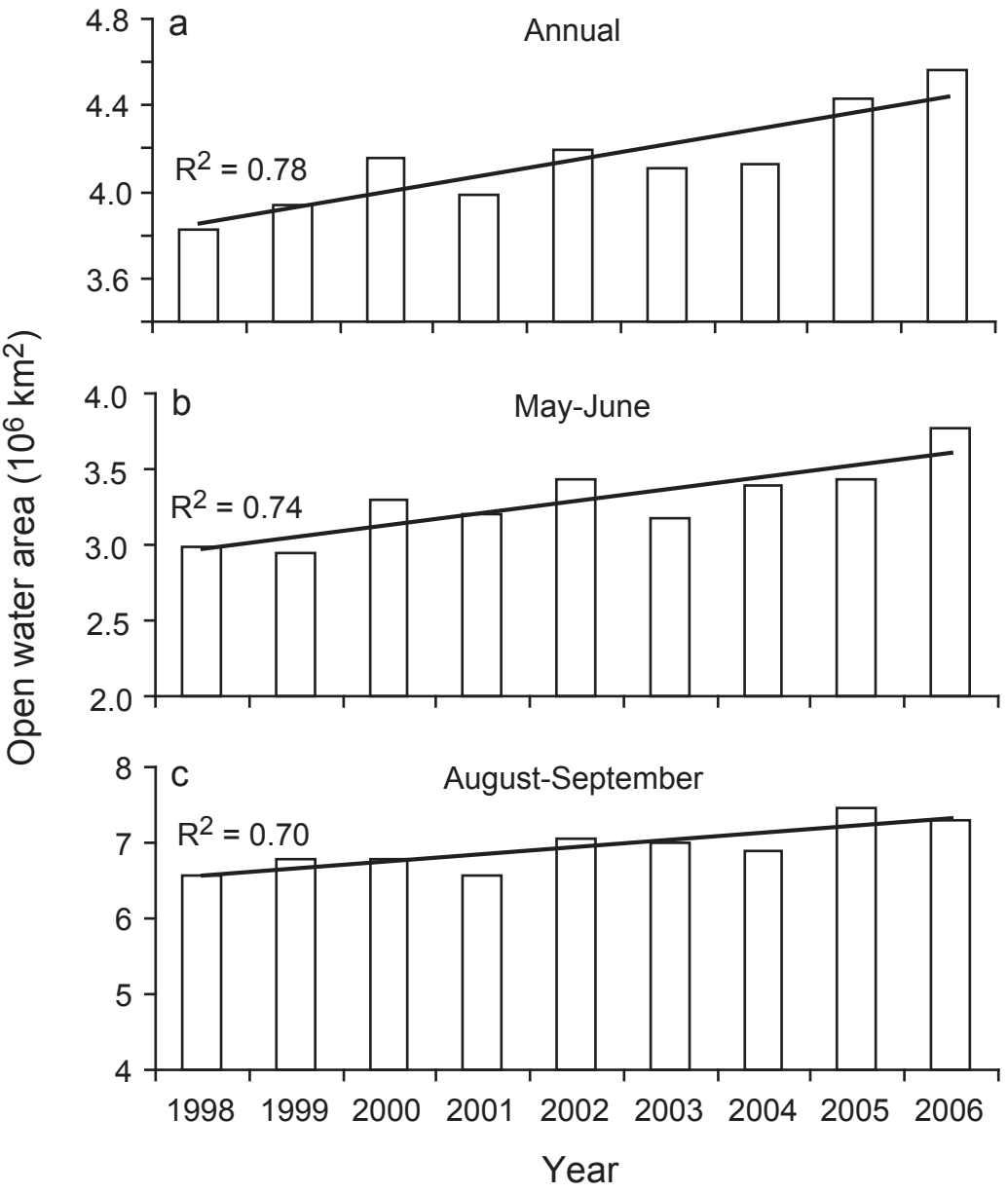
a
Annual
4.8
4.4
4.0
3.6
R2 = 0.78
b
May-June
4.0
3.5
3.0
2.5
2.0
R2 = 0.74
c
August-September
8
7
6
5
4
R2 = 0.70
1998
1999
2000
2001
2002
2003
2004
2005
2006
Year
Open water area (10^6 km^2)

Figure 3

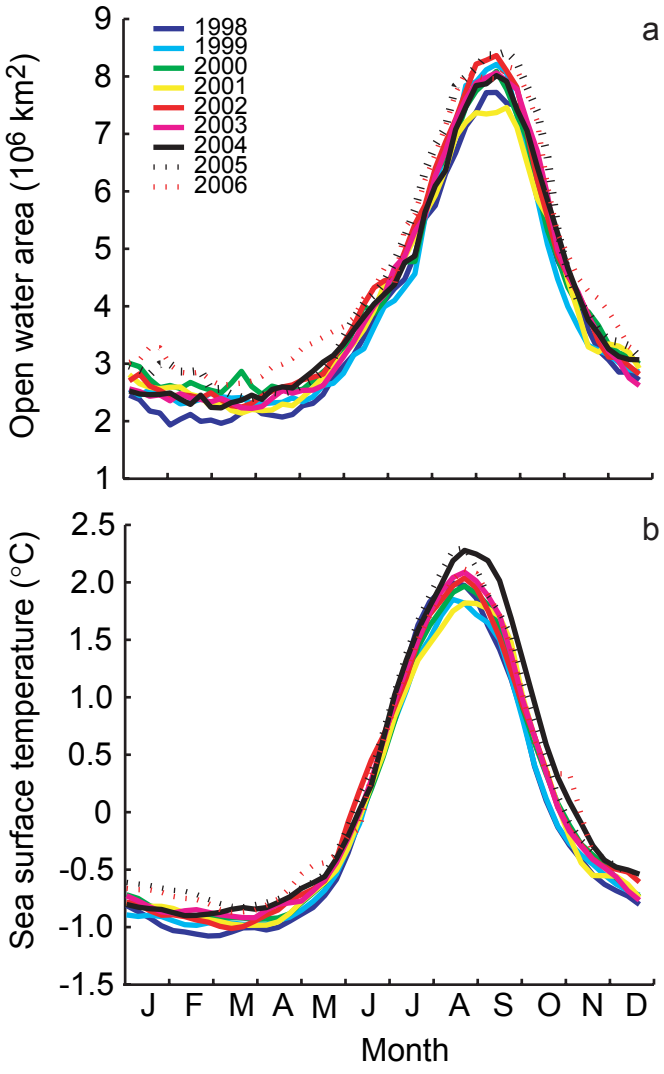
a
b
1998
1999
2000
2001
2002
2003
2004
2005
2006
Open water area (10^6 km^2)
Sea surface temperature (°C)
9
8
7
6
5
4
3
2
1
2.5
2.0
1.5
1.0
0.5
0
-0.5
-1.0
-1.5
J F M A M J J A S O N D
Month

Figure 4

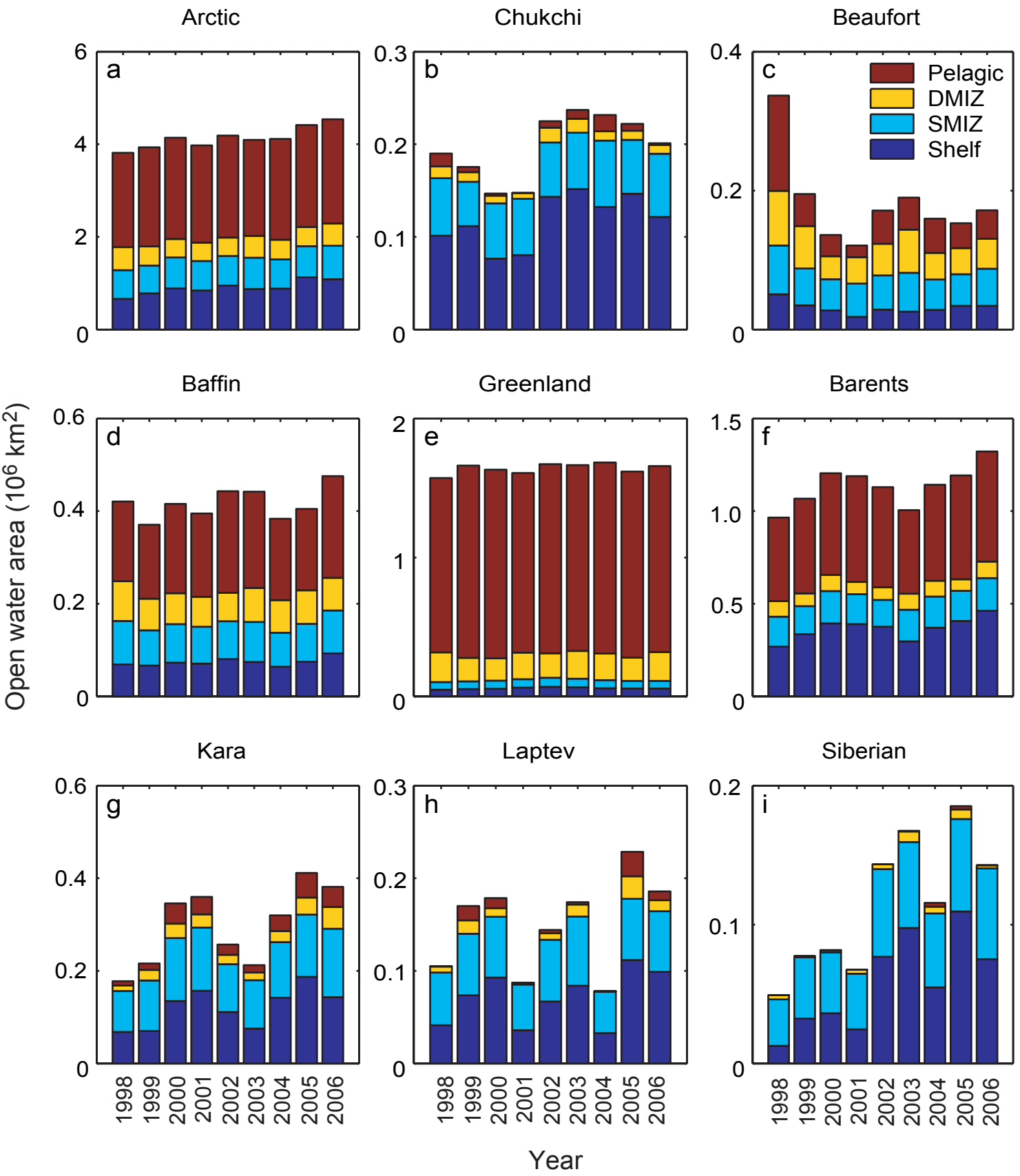
Arctic
Chukchi
Beaufort
Baffin
Greenland
Barents
Kara
Laptev
Siberian
a
b
c
d
e
f
g
h
i
Pelagic
DMIZ
SMIZ
Shelf
Open water area (10^6 km^2)
Year
1998
1999
2000
2001
2002
2003
2004
2005
2006

Figure 5

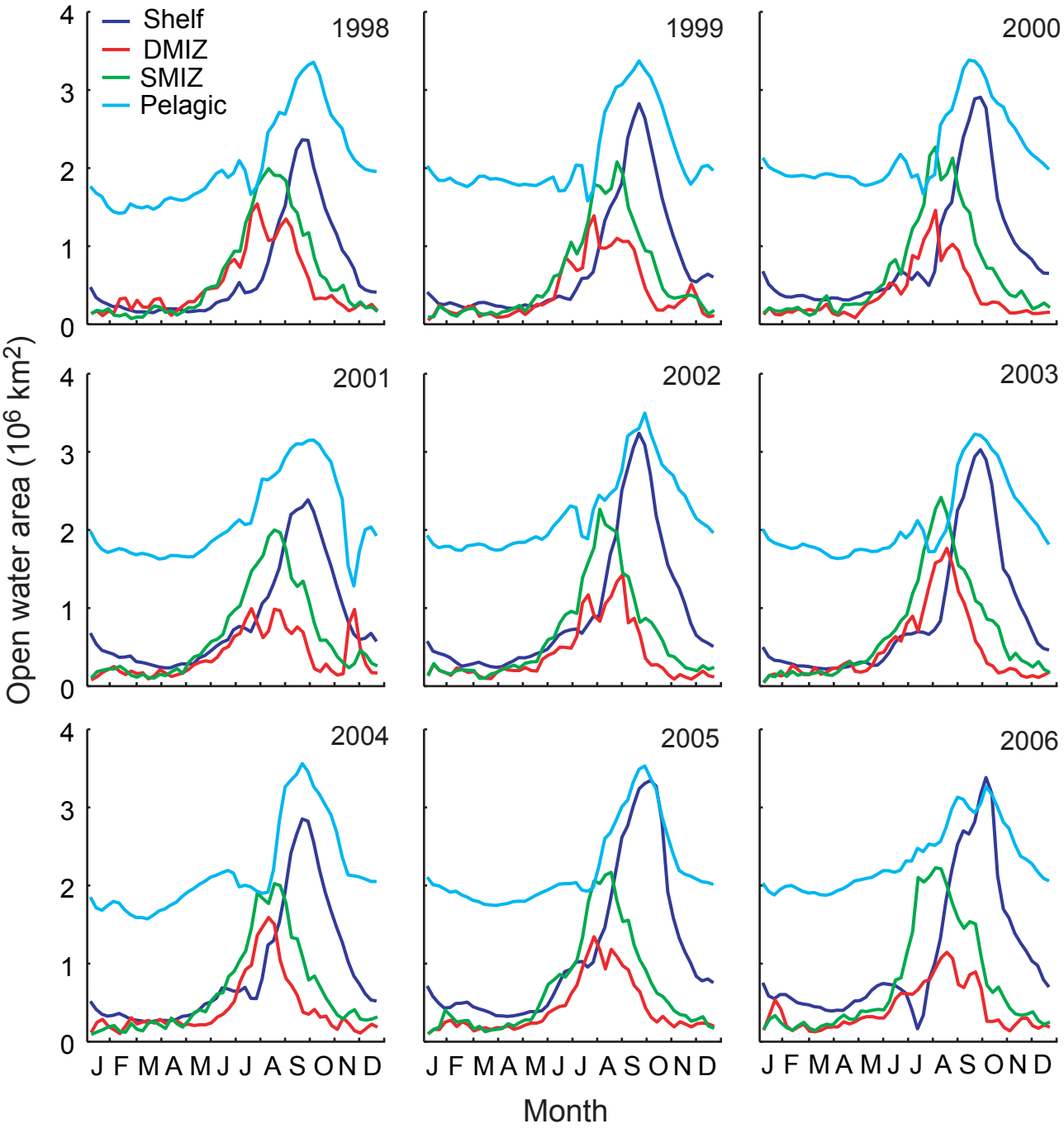
Shelf
DMIZ
SMIZ
Pelagic
1998
1999
2000
2001
2002
2003
2004
2005
2006
Open water area (10^6 km^2)
0
1
2
3
4
J F M A M J J A S O N D
Month

Figure 6

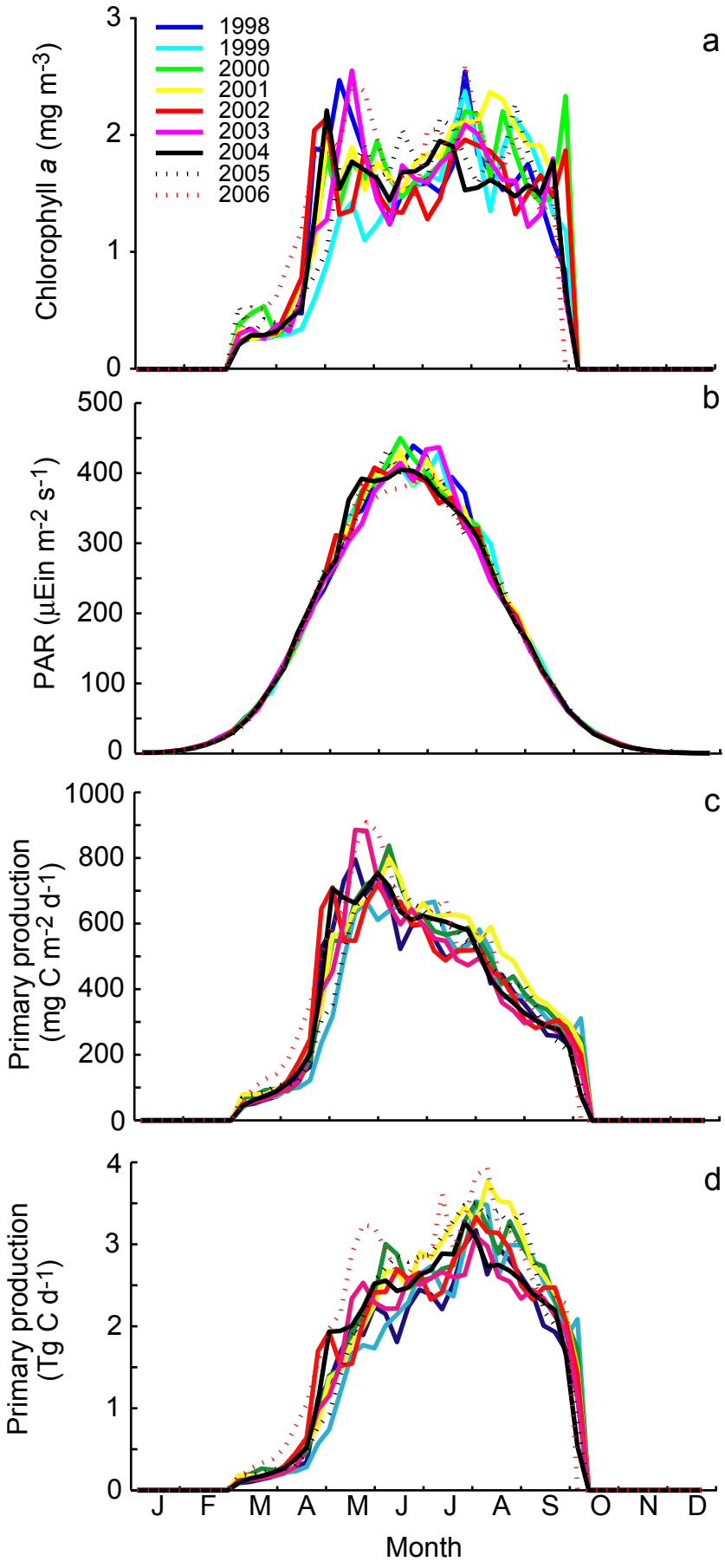
a
b
c
d
Chlorophyll a (mg m-3)
PAR (µEin m-2 s-1)
Primary production (mg C m-2 d-1)
Primary production (Tg C d-1)
1998
1999
2000
2001
2002
2003
2004
2005
2006
J F M A M J J A S O N D
Month

Figure 7

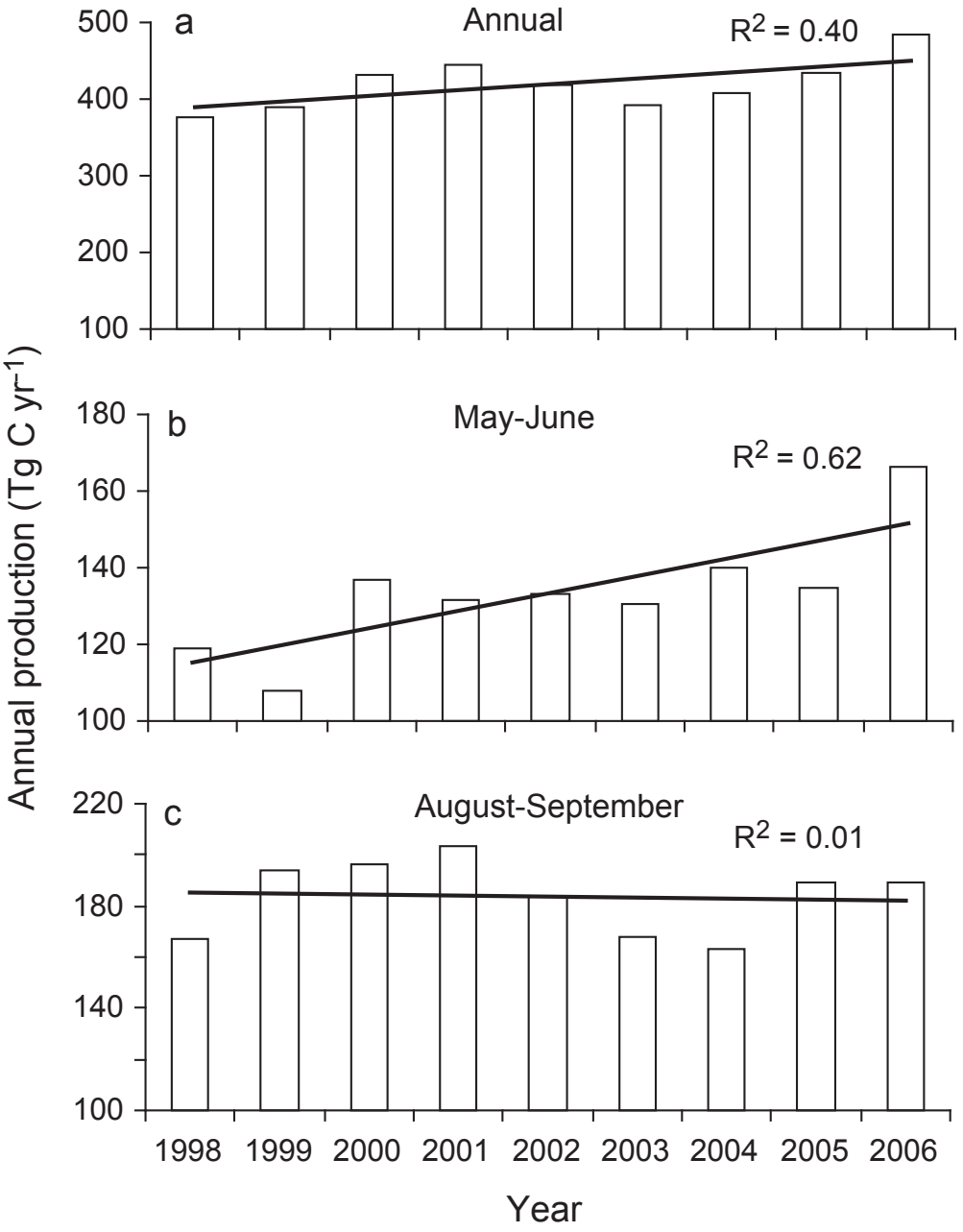
a
Annual
R^2 = 0.40
500
400
300
200
100
b
May-June
R^2 = 0.62
180
160
140
120
100
c
August-September
R^2 = 0.01
220
180
140
100
1998
1999
2000
2001
2002
2003
2004
2005
2006
Year
Annual production (Tg C yr^{-1})

Figure 8

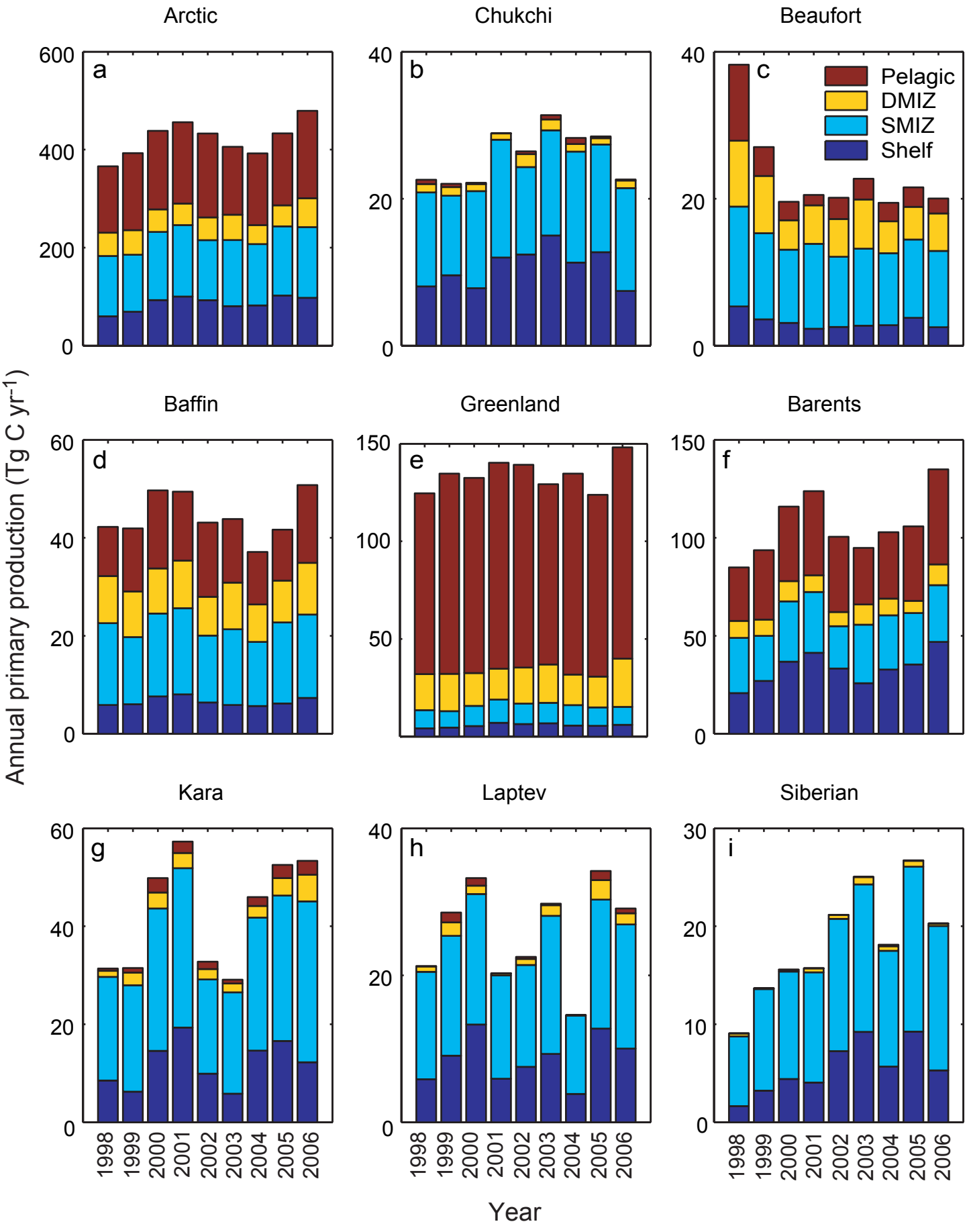
Arctic
Chukchi
Beaufort
Baffin
Greenland
Barents
Kara
Laptev
Siberian
a
b
c
d
e
f
g
h
i
Pelagic
DMIZ
SMIZ
Shelf
Annual primary production (Tg C yr-1)
Year
1998
1999
2000
2001
2002
2003
2004
2005
2006

Figure 9

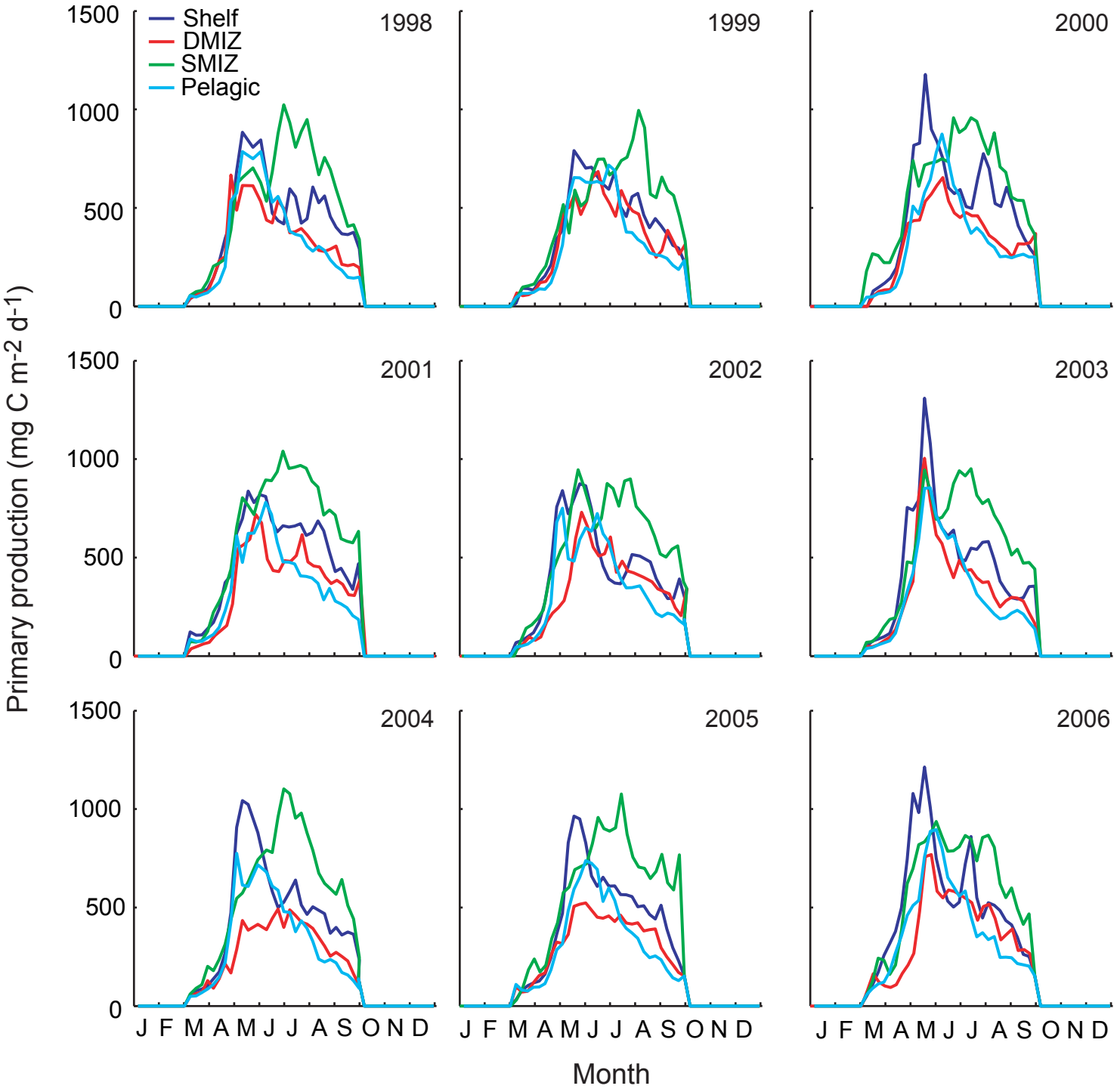
Shelf
DMIZ
SMIZ
Pelagic
1998
1999
2000
2001
2002
2003
2004
2005
2006
1500
1000
500
0
Primary production (mg C m-2 d-1)
J F M A M J J A S O N D
Month

Figure 10

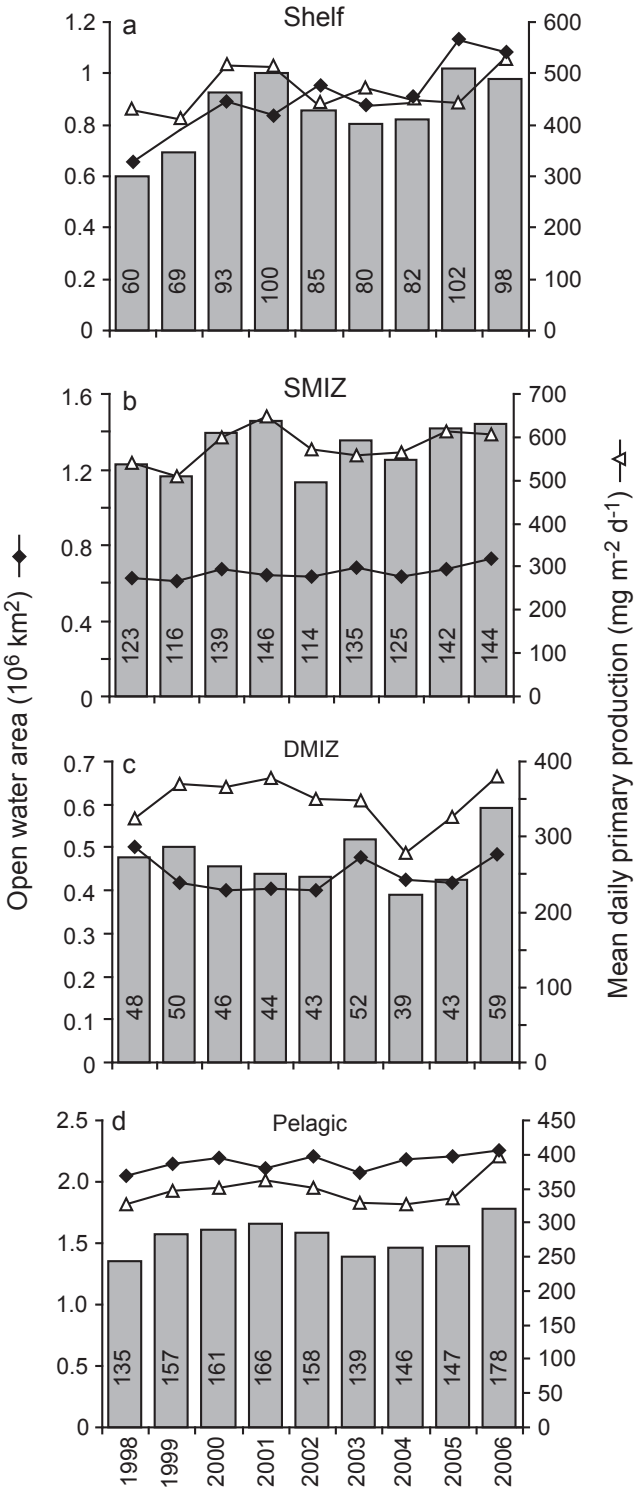
a
Shelf
b
SMIZ
c
DMIZ
d
Pelagic
Open water area (10^6 km^2)
Mean daily primary production (mg m^-2 d^-1)
60
69
93
100
85
80
82
102
98
123
116
139
146
114
135
125
142
144
48
50
46
44
43
52
39
43
59
135
157
161
166
158
139
146
147
178
1998
1999
2000
2001
2002
2003
2004
2005
2006

Figure 11

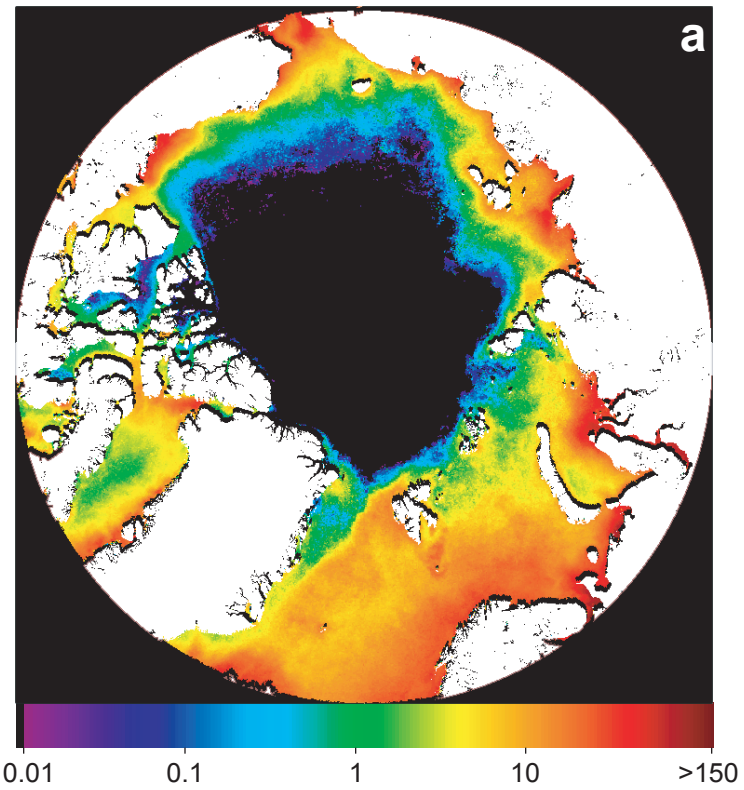

Annual primary production (g C m^{-2} yr^{-1})

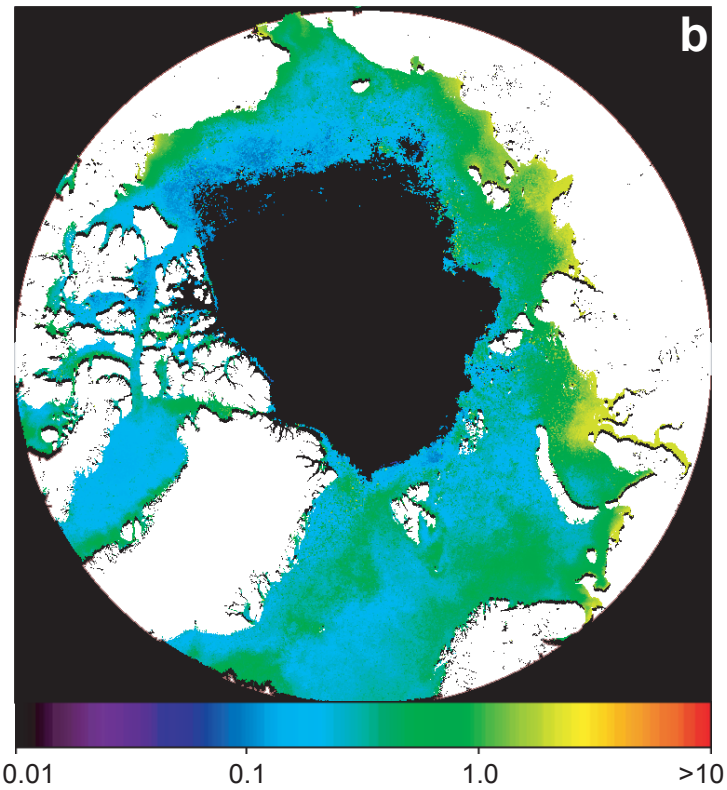

Annual mean chlorophyll *a* (mg m^{-3})

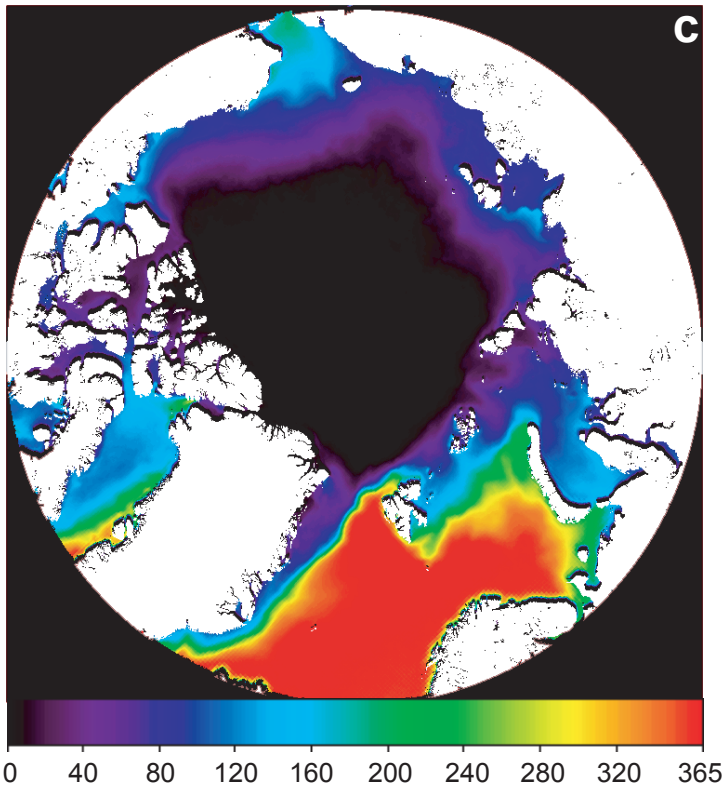

Annual open water (days not ice covered)

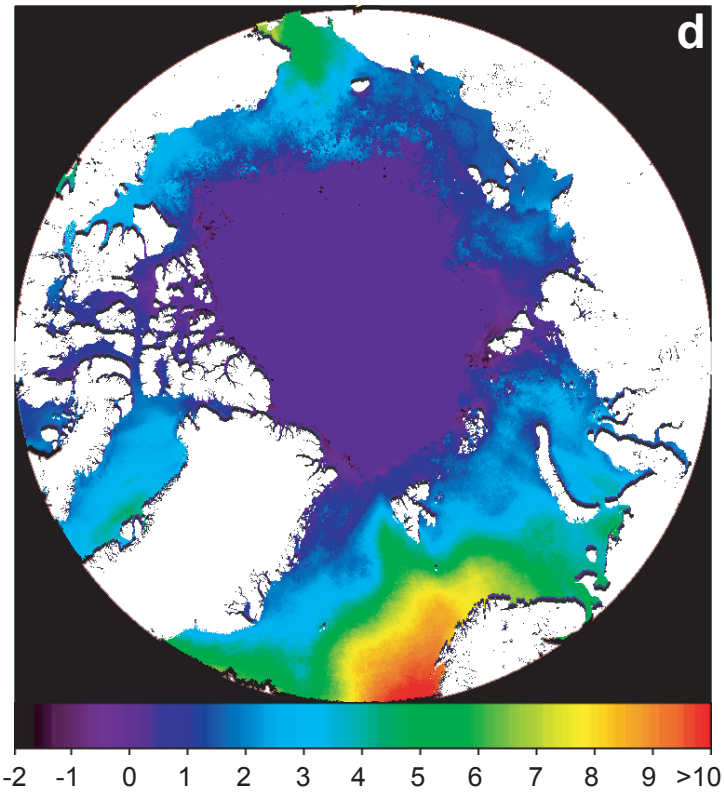

Annual mean SST (°C)

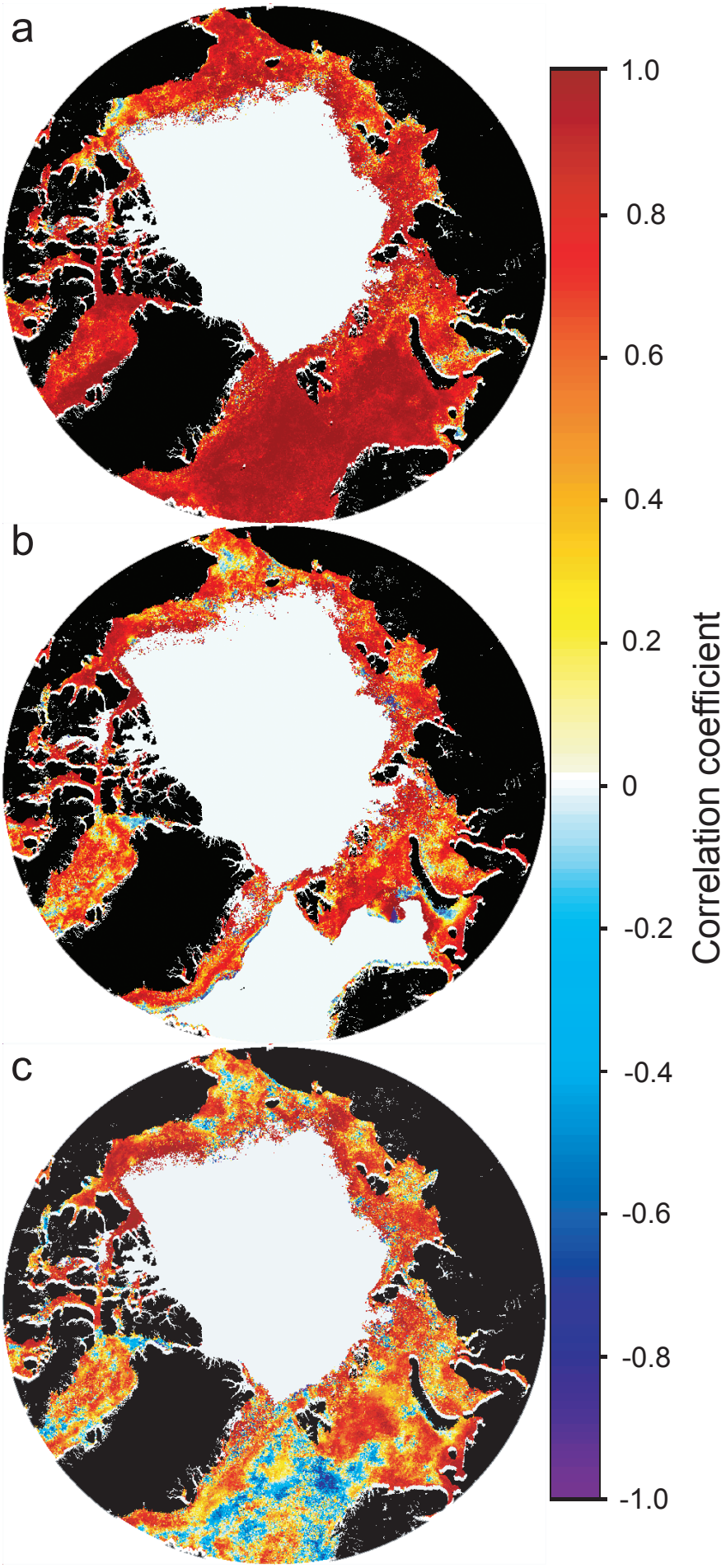

Figure 13

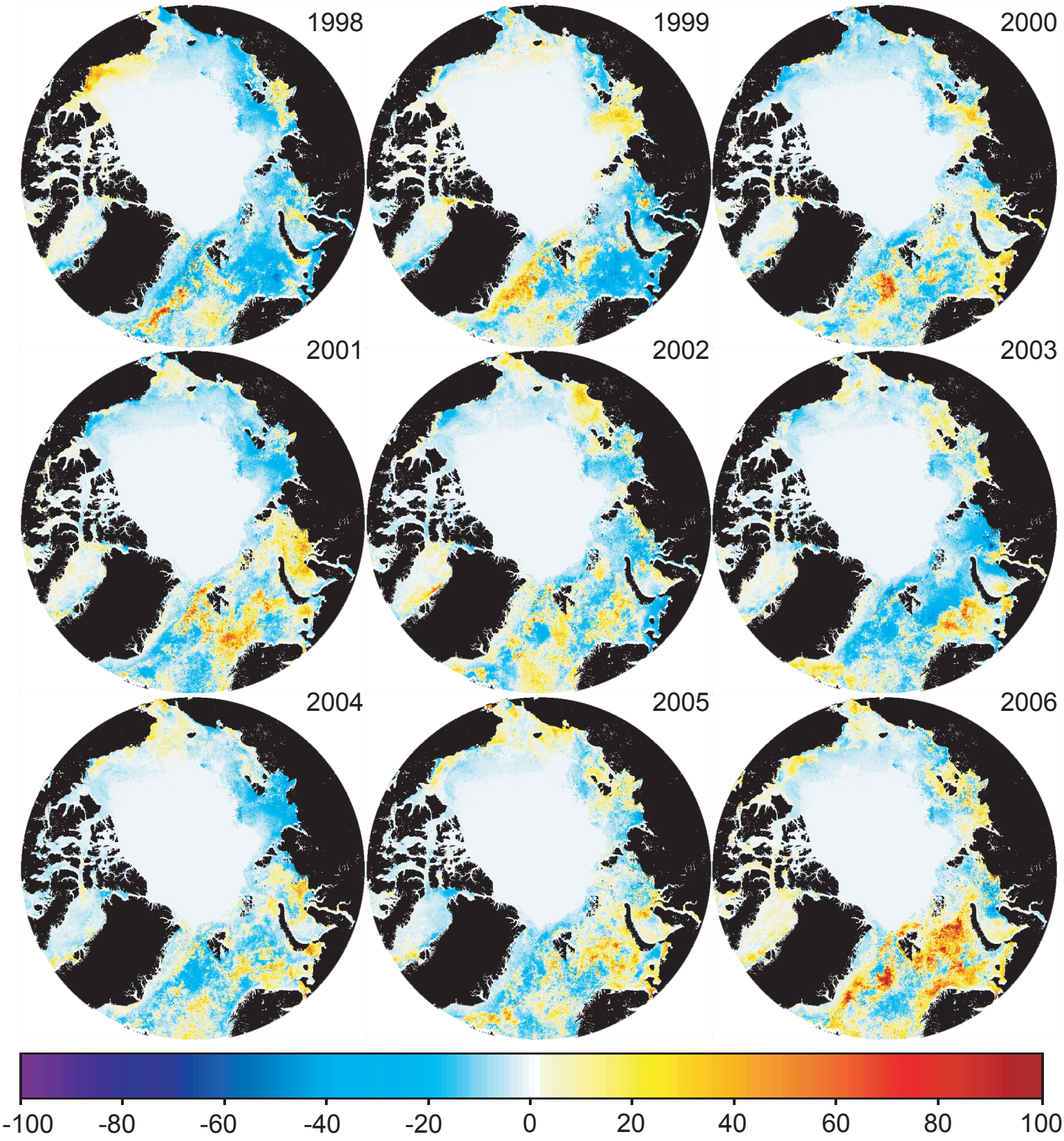
1998
1999
2000
2001
2002
2003
2004
2005
2006
-100
-80
-60
-40
-20
0
20
40
60
80
100
Annual primary production anomalies (g C m-2 yr-1)

Figure 14

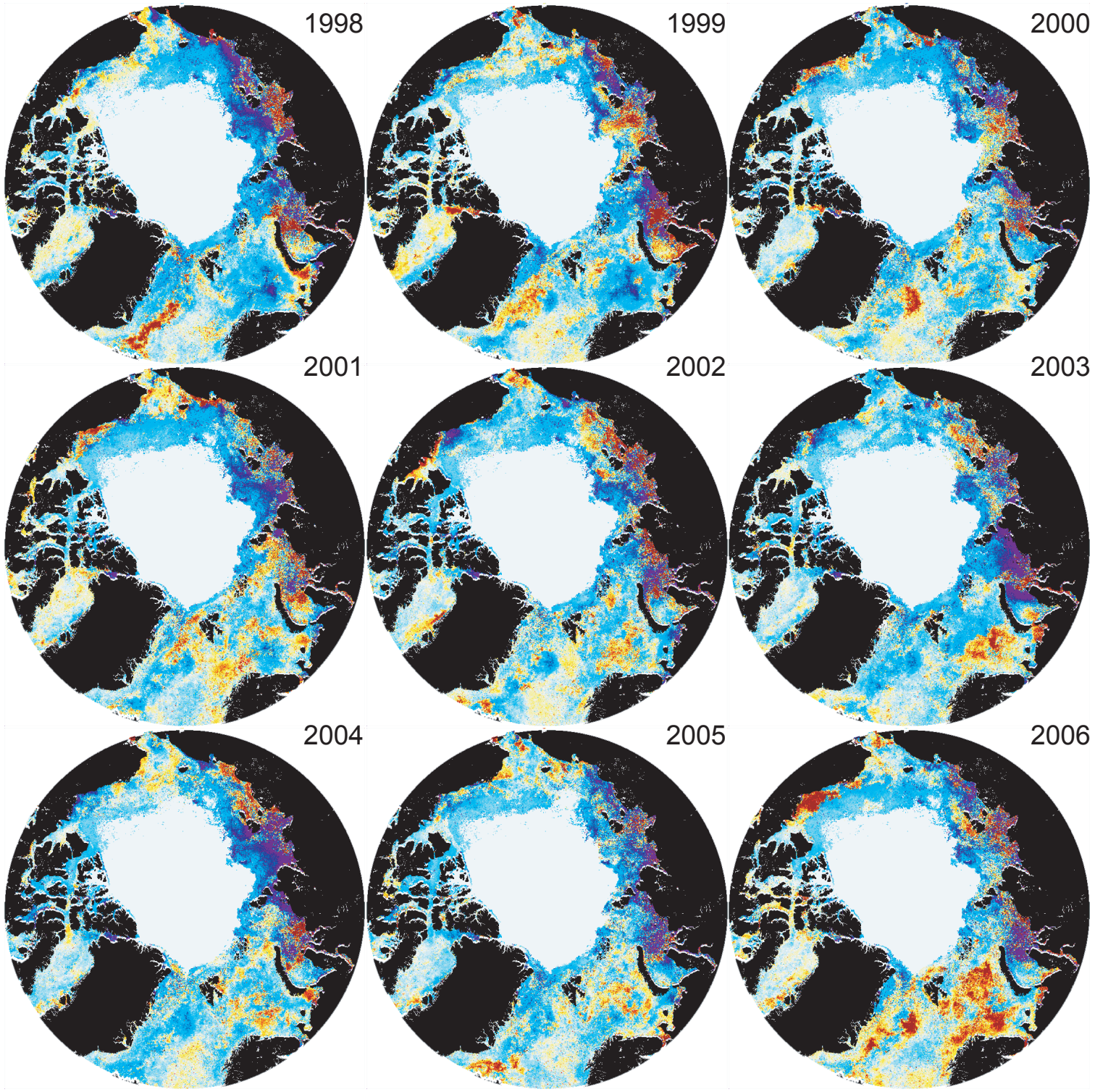
1998
1999
2000
2001
2002
2003
2004
2005
2006
-2.0
-1.6
-1.4
-0.8
-0.4
0
0.4
0.8
1.2
1.6
2.0
Chlorophyll a anomalies (mg m-3)

Figure 15

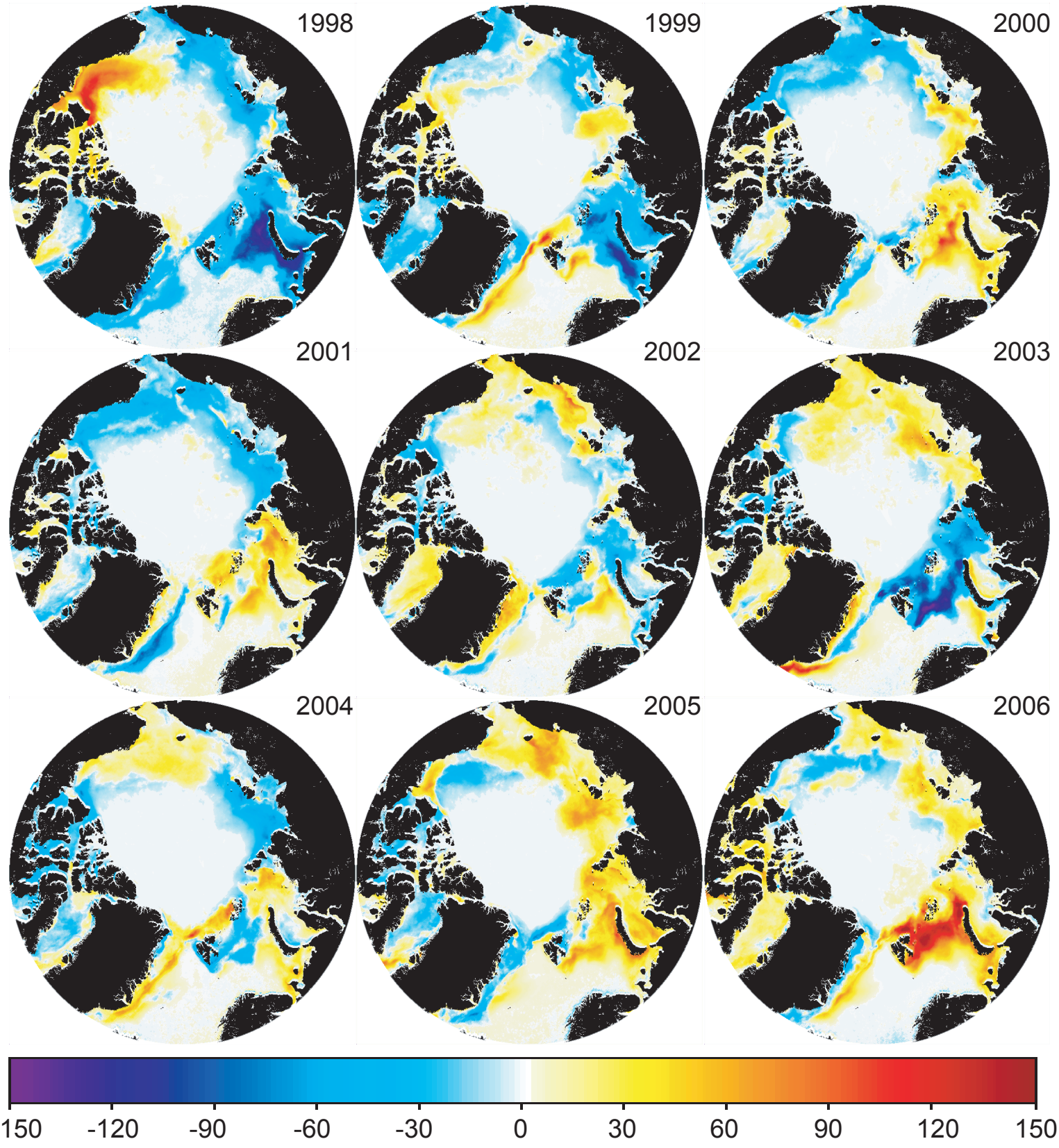
1998
1999
2000
2001
2002
2003
2004
2005
2006
-150
-120
-90
-60
-30
0
30
60
90
120
150
Open water anomalies (number of days with open water)

Figure 16

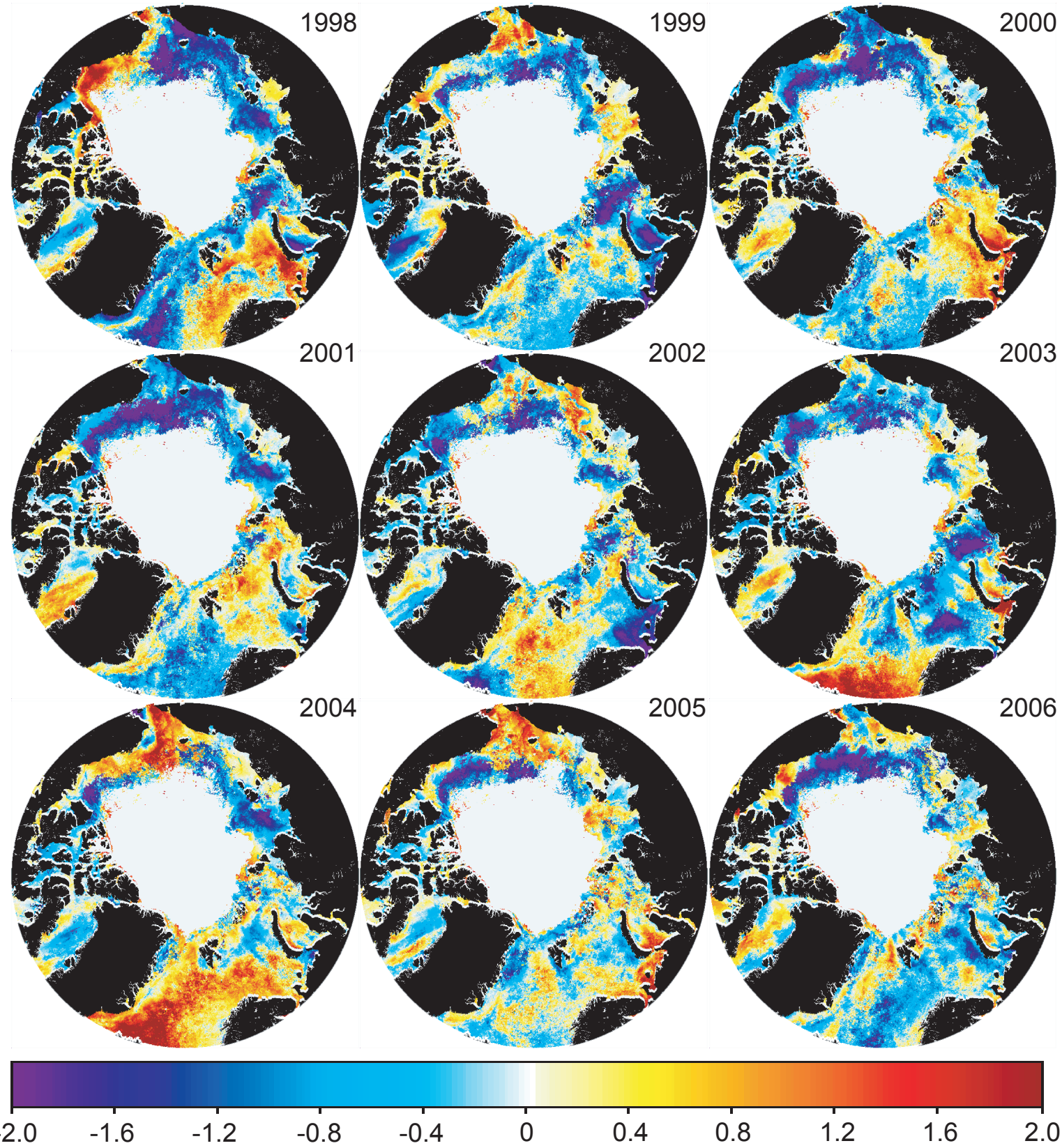
1998
1999
2000
2001
2002
2003
2004
2005
2006
-2.0
-1.6
-1.2
-0.8
-0.4
0
0.4
0.8
1.2
1.6
2.0
Sea surface temperature anomalies (°C)

Figure 17

Table 1. Linear Regression of Open Water Area Against Year by Geographic Sector and Ecological Province.

	Chukchi	Beaufort	Baffin	Greenland	Barents	Kara	Laptev	Siberian	Arctic
Shelf									
Slope*	6131	-967	1762	898	14190	9711	4552	**9841**	**46110**
R^2	0.360	0.089	0.320	0.135	0.436	0.394	0.186	**0.635**	**0.768**
p-value	0.087	0.435	0.113	0.330	0.053	0.070	0.246	**0.010**	**0.002**
SMIZ									
Slope*	1328	-1425	19	102	1398	4202	288	**3937**	**9848**
R^2	0.298	0.225	0.000	0.005	0.145	0.336	0.007	**0.751**	**0.546**
p-value	0.128	0.197	0.984	0.850	0.312	0.102	0.833	**0.002**	**0.023**
DMIZ									
Slope*	-24	-2966	-563	523	332	2578	743	441	1063
R^2	0.000	0.284	0.049	0.006	0.007	0.431	0.081	0.262	0.005
p-value	0.956	0.140	0.568	0.848	0.832	0.055	0.459	0.159	0.850
Pelagic									
Slope*	-35	-5816	3872	4810	9138	3555	809	198	16529
R^2	0.000	0.216	0.237	0.101	0.247	0.391	0.061	0.250	0.415
p-value	0.965	0.207	0.184	0.405	0.174	0.072	0.520	0.170	0.061
Total									
Slope*	7399	-11174	5090	6333	25047	20046	6392	**14416**	**73550**
R^2	0.339	0.238	0.180	0.225	0.390	0.425	0.120	**0.680**	**0.780**
p-value	0.100	0.183	0.256	0.197	0.072	0.057	0.361	**0.006**	**0.002**

Bold denotes statistical significance at the 95% confidence level.

*Slopes are in units of $km^2\ yr^{-1}$

Table 2. Linear Regression of Annual Primary Production Against Open Water Area by Geographic Sector

	Chukchi	Beaufort	Baffin	Greenland	Barents	Kara	Laptev	Siberian	Arctic
Slope*	5.33	**9.17**	6.75	9.84	**13.4**	**12.7**	**12.4**	**11.3**	**12.1**
R^2	0.269	**0.895**	0.24	0.15	**0.866**	**0.893**	**0.896**	**0.942**	**0.617**
p-value	0.153	**<0.001**	0.181	0.304	**<0.001**	**<0.001**	**<0.001**	**<0.001**	**0.012**

Bold denotes statistical significance at the 95% confidence level.

*Slopes are in units of (10^7 g C yr^{-1}) km^{-2}

Table 3. Linear Regression of Annual Primary Production Against Year by Geographic Sector and Ecological Province.

	Chukchi	Beaufort	Baffin	Greenland	Barents	Kara	Laptev	Siberian	Arctic
Shelf									
Slope*	0.280	-0.183	0.000	0.170	1.783	0.539	0.204	**0.673**	3.466
R^2	0.087	0.278	0.000	0.220	0.365	0.099	0.031	**0.500**	0.438
p-value	0.442	0.145	0.998	0.203	0.085	0.409	0.650	**0.033**	0.052
SMIZ									
Slope*	0.308	-0.289	0.002	0.041	0.077	0.917	0.057	**0.924**	2.038
R^2	0.266	0.397	0.000	0.011	0.004	0.220	0.004	**0.738**	0.205
p-value	0.155	0.069	0.992	0.788	0.870	0.203	0.875	**0.003**	0.221
DMIZ									
Slope*	-0.009	-0.389	-0.029	0.314	-0.005	0.281	0.078	0.038	0.278
R^2	0.007	0.390	0.008	0.080	0.000	0.399	0.070	0.245	0.016
p-value	0.833	0.072	0.822	0.460	0.980	0.068	0.491	0.175	0.747
Pelagic									
Slope*	-0.010	-0.593	0.071	0.592	1.173	0.178	0.000	0.007	1.417
R^2	0.012	0.373	0.007	0.054	0.239	0.268	0.000	0.141	0.080
p-value	0.781	0.081	0.830	0.549	0.182	0.153	0.999	0.319	0.461
Total									
Slope*	0.576	-1.445	0.076	1.188	3.066	1.938	0.352	**1.648**	7.892
R^2	0.193	0.421	0.002	0.122	0.279	0.218	0.021	**0.647**	0.334
p-value	0.237	0.059	0.906	0.357	0.144	0.205	0.709	**0.009**	0.103

Bold denotes statistical significance at the 95% confidence level.

*Slopes are in units of (Tg C yr^{-1}) yr^{-1}